

Computational Advances in Ionic Liquid-Mediated Extractive Desulfurization of Fuel: A Minireview

Robert Wilson-Kovacs and Orlando Acevedo*

Department of Chemistry, University of Miami, Coral Gables, Florida 33146, United States

E-mail: orlando.acevedo@miami.edu

Submitted August 12, 2024

Abstract: Removing sulfur compounds from petroleum is essential in mitigating harmful emissions linked to fuel combustion. Problematically, thiophenic compounds that are readily present in fossil fuels resist conventional desulfurization methods. Extractive Desulfurization (EDS) provides an attractive alternative that can be selective for heterocyclic sulfur compounds, i.e., thiophene and its derivatives, through the choice of solvent employed. To this end, a burgeoning field has developed around the use of ionic liquids (ILs) given their ability to be fine-tuned with varying levels of polarity and solubility to suit the specific requirements of the desulfurization process. Hundreds of experimental studies featuring the use of IL technologies have provided encouraging trends for the design of more efficient extractants; however, conflicting data and a lack of a definitive understanding of important solute-ion interactions has presented challenges in advancing the field. More recently, computational investigations have been employed to unravel these key interactions and to inform design principles for future high-performance IL extractants. The myriad of intermolecular forces, e.g., coulombic, dispersive, and steric, and their subtle interplay present in IL-mediated EDS processes are prime for study using computational methodologies that include quantum mechanics (QM) at the ion-solute interaction level, molecular dynamics (MD) for the simulation of bulk-phase solvent properties, and the Conductor-Like Screening Model (COSMO) for high-throughput screening. This minireview summarizes computational advances and findings in the field of IL-mediated EDS in a format suitable for theoreticians and experimental chemists alike with discussions provided of future directions for the field.

1. Introduction

Contemporary conversations regarding the environmental consequences of burning fossil fuels have primarily focused on the emission of carbon dioxide (CO₂) and its contribution to climate change.¹ Nevertheless, the devastating impact of sulfur dioxide (SO₂) pollution, another byproduct of fossil fuel combustion, should not be underestimated. For example, the World Health Organization (WHO) estimates that air pollution kills 7 million people annually,² largely in developing countries, in major part due to respiratory diseases derived from SO₂ and its characteristic smog.³ Additional environmental impacts of anthropogenic SO₂ pollution include acid rain and global dimming, that has negatively impacted soil quality and plant growth, has disrupted both terrestrial and aquatic ecosystems, and has led to a decrease in total surface irradiation by around 2-5% per decade between the 1950s and 1990s.⁴ Consequently, developing efficient, cost-effective, and scalable solutions to reduce sulfur emissions during fuel combustion is a key priority in safeguarding human health and environmental integrity.

Fuel oil serves as the primary energy source for global consumption and ranks as the second-largest contributor to SO₂ pollution, following coal combustion.⁵ Crude oil, the source of fuel oil, contains up to 7.89 percent sulfur by mass content, making it the most abundant heteroatom in crude mixtures.⁶ A wide range of sulfur-containing compounds are present, from elemental sulfur and hydrogen sulfide (H₂S) to organic compounds such as thiols, sulfides, and thiophenes (Figure 1) that require different removal processes to meet mandated environmental and fuel product quality standards.⁷ Currently, the industry-standard process for the desulfurization of fossil fuels is hydrodesulfurization (HDS), which involves the catalyzed reaction of sulfur impurities with hydrogen gas (H₂) at high temperatures and pressures.⁸ Unfortunately, thiophene and derivatives have proven particularly challenging to remove due to similar chemical properties with other hydrocarbons present in the crude mixtures, e.g., comparable boiling points impede the distillation process, and strong aromatic bonds and the

low electron density of the sulfur atom resist conventional oxidative desulfurization methods. HDS can remove these refractory sulfur compounds but requires harsher conditions and higher temperatures that can lead to reduced octane ratings in purified fuel and the formation of toxic H₂S byproducts.⁹ As such, alternative non-HDS desulfurization processes, including biological desulfurization (BDS), oxidative desulfurization (ODS), adsorption desulfurization (ADS), and extractive desulfurization (EDS) have been explored.⁹

Table 1. Published Review Articles (2014 to 2024) Pertaining to Ionic Liquid-Mediated Extractive Desulfurization.

Areas of Focus	Year	Ref
Application of ionic liquids (ILs) in extractive and oxidative desulfurization (EDS and ODS)	2024	¹⁰
Evaluation of desulfurization and denitrogenation methodologies (including ODS and EDS) with some discussion of ILs	2024	¹¹
Bibliometric mapping of ILs in fuel oil desulfurization, including EDS and ODS	2024	¹²
Examination of adsorption materials for fuel desulfurization, including IL-EDS	2024	¹³
Overview of metal-based ILs for EDS and ODS	2024	¹⁴
Comparison between ILs and deep eutectic solvents (DESs) for EDS	2023	¹⁵
Application of ILs to desulfurization including EDS and ODS	2022	¹⁶
Comparison between ILs and DESs for EDS of middle distillate fuels	2022	¹⁷
Mechanisms of IL-mediated EDS and ODS	2022	¹⁸
Metal-free ODS of fuels with a discussion of IL-ODS	2022	¹⁹
Desulfurization and denitrogenation methods with a focus on ILs and EDS	2021	²⁰
ILs and DESs for the desulfurization of biodiesel, bioethanol, and hydrogen fuels	2021	²¹
DES-mediated EDS of model and real fuels with comparisons to ILs	2021	²²
Factors affecting ODS efficiency and development with a section on IL-ODS	2021	²³
ODS of fuels using polyoxometalate (POM)-based catalysts, including POM-ILs	2021	²⁴
Desulfurization and denitrogenation of model fuels and real fuels using ILs	2019	²⁵
Alternatives to hydrodesulfurization (HDS) of fuels with special emphasis on ILs	2017	²⁶
Metal-containing ILs, including their applications in IL-EDS and IL-ODS of fuels	2017	²⁷
EDS of fuel oils, including green alternatives with a section on IL-EDS	2017	²⁸
Comprehensive discussion of IL-EDS for both model oils and fuel oils	2014	²⁹

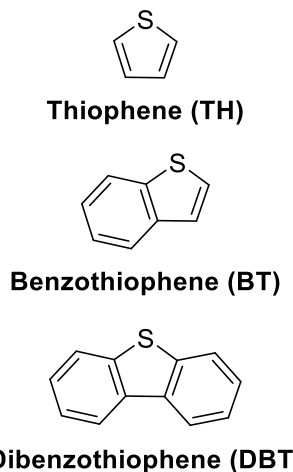


Figure 1. Sulfur compounds present in fuel and diesel oil explored within this review.

Among these varied desulfurization techniques, EDS has garnered significant attention given several inherent methodological advantages that include mild pressures and temperatures, no oxidants/catalysts utilized, low cost, and no H₂ consumption needed. Instead, sulfur compounds are selectively removed from fuel oils using extractant solvents that are unreactive with the desirable hydrocarbons.²⁹ However, the choice of extractant is incredibly important as many conventional solvents (e.g., DMF, CH₃CN, and DMSO) contain severe drawbacks such as volatility, toxicity, low selectivity, and fuel contamination.³⁰ Fortunately, environmentally friendly and cost-effective alternative solvents in the form of ionic liquids (ILs) have proven to be highly promising candidates for EDS.^{16, 26, 29} ILs are solvents comprised exclusively of ions that often melt near room temperature and exhibit a wide range of industrially desirable properties, including recyclability and air/water stability.³¹ While the number of possible cationic and anionic species available for IL design is nearly limitless,³² the most commonly utilized classes for desulfurization feature large asymmetric cations based on imidazolium and pyridinium (Figure 2) coupled to small, diffuse, inorganic anions, such as tetrafluoroborate (BF₄) and hexafluorophosphate (PF₆).

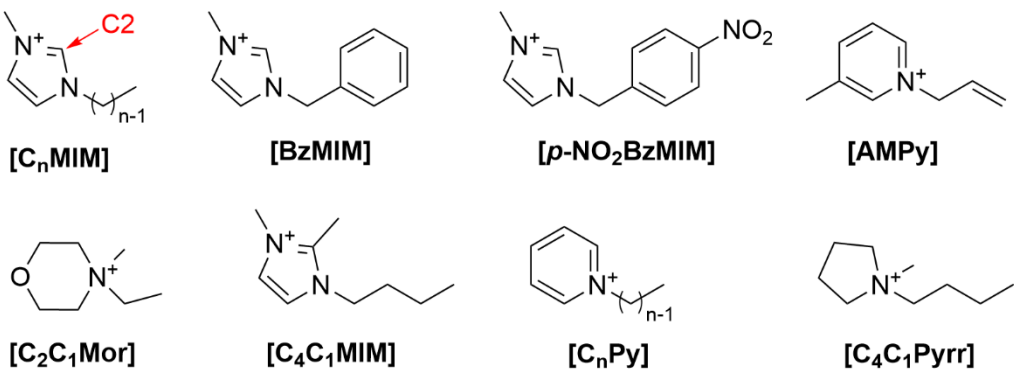


Figure 2. Examples of IL cations explored in this minireview. Their nomenclature has been standardized throughout the text using the assigned bold script. The C2 carbon in [C_nMIM] is highlighted in red.

The ability of ILs to remove refractory sulfur compounds from fuel was first established by Jess and co-workers in 2001³³ and has since been examined in hundreds of experimental studies over the past two decades.³⁴ Table 1 compiles a list of detailed review articles from the past ten years that cover the many findings that have advanced both the knowledge and design of more efficient IL extractants. However, a glaring omission in the literature is the lack of a review article that highlights the significant progress made in this field using computational approaches. This timely minireview critically examines numerous computational studies spanning back over 15 years that have helped elucidate the origin of enhanced fuel desulfurization using ILs. An overview and evaluation of the simulations, methods, and parameters is provided that includes quantum mechanical (QM) calculations (**Section 2**), molecular dynamics (MD) simulations (**Section 3**), and the Conductor-Like Screening Model for Realistic Solvents (COSMO-RS) thermodynamic model (**Section 4**). Corroboration between computational findings and their relation to experimental trends, as well as perspectives as to the most fruitful avenues for further computational research into this challenging topic are also given. This minireview is intended for both computational chemists who wish to better understand the state-of-the-art methodologies used to perform simulations

of IL-mediated EDS and for experimentalists who are interested in the computationally driven design principles of these IL species. While this minireview cannot be exhaustive given the page limitations, key findings are highlighted while attempting to reconcile this corpus of literature into a thorough and easily accessible evaluation of the current field alongside prognostication of future developments (**Section 5**) that include employing methods such as coarse-grained molecular dynamics (CGMD) and ab initio molecular dynamics (AIMD).

2. Quantum Mechanical (QM) Calculations

2.1. QM Introduction

Theoretical studies on ionic liquid-driven extractive desulfurization have depended heavily on quantum mechanical (QM) modeling to explain the physical, structural, and thermodynamical relationships present between solvent ions and refractory sulfur compounds. The reported investigations explored in this section primarily employed density functional theory (DFT) methods, such as B3LYP^{35, 36} and M06-2X,³⁷ given the computationally prohibitive nature of wave function-based electron correlation methods, such as perturbation theory (e.g. MP2) and configuration interaction (CI), when treating the large number of heavy atoms present in IL complexes.³⁸ As this section covers single-state calculations and optimizations, the scope of these computational reports revolved around the exploration of two key phenomena: the nature of binding between IL and refractory sulfur complexes at their geometry-optimized, local energy minima (Section 2.2 with a summary provided in Table 2), and the transition states that correspond to the IL-catalyzed oxidation pathway of TH/DBT compounds (Section 2.3 with a summary provided in Table 3).

Table 2. Key Findings of Ionic Liquid-Mediated Extractive Desulfurization Derived from Quantum Mechanical Calculations.

Year	QM Method	Ions Examined	Key Findings	Ref.
2012	GGA/PW91/DNP	$[\text{C}_n\text{MIM}]$ ($n = 1, 4$), $[\text{PF}_6^-], [\text{BF}_4^-]$	Adsorption of TH by IL was dominated by cation- $\text{H}^\cdot\pi(\text{TH})$ and $(\text{TH})\text{H}^\cdot\text{F}$ -anion interactions.	³⁹
2012	GGA/PW91/DNP	$[\text{C}_1\text{MIM}], [\text{MeSO}_4^-]$	Adsorption of DBT controlled by weak $\pi\text{-}\pi$ interactions, $\text{C-H}^\cdot\pi$ interactions, and hydrogen bonding.	⁴⁰
2014	$\omega\text{B97X-D/6-31++G(d,p)}$	$[\text{C}_4\text{Py}], [\text{HSO}_4^-]$	Adsorption of TH/DBT dominated by strong $\pi\text{-}\pi$ interactions, whereas THO_2 & DBTO_2 have weaker $\pi\text{-}\pi$ interactions but stronger interaction energies from greater sulfone nucleophilicity.	⁴¹
2015	M06-2X/6-31++G(d,p), SMD-GIL continuum solvent	$[\text{C}_4\text{MIM}], [\text{AlCl}_4^-], [\text{Al}_2\text{Cl}_7^-]$	Energy interactions with metal-based ILs followed $\text{TH} < \text{BT} < \text{DBT}$. Steric interactions, polarization, and charge transfer accounted for 55%, 25%, and 18% of the energy. $\text{C-H}^\cdot\pi$ interactions were insignificant.	⁴²
2017	B3LYP/6-31G(d,p)	$[\text{C}_n\text{MIM}]$ ($n = 2, 4, 6, 8$), $[\text{BF}_4^-]$	Increasing alkyl chain length in $[\text{C}_n\text{MIM}]$ improved interaction energy and increased the number of hydrogen bonds with DBT. Dominant $\pi\text{-}\pi$ stacking and $\text{C-H}^\cdot\pi$ interactions also present. Anion played only a complementary role.	⁴³
2019	B3LYP/6-31++G(d,p), IEFPCM continuum solvent	$[\text{BzMIM}], [\text{o/m/p-NO}_2\text{BzMIM}], [\text{Br}]$	Electron-withdrawing nature of the NO_2 group creates a more electron-poor imidazolium cation for improved TH binding. Improved extraction efficiency is a function of strong inductive effects and low steric crowding.	⁴⁴
2019	AFPD, PCM continuum solvent	$[\text{C}_n\text{MIM}]$ ($n = 2, 4, 6, 8, 10$), $[\text{C}_4\text{Py}], [\text{C}_4\text{C}_1\text{MIM}], [\text{C}_4\text{C}_1\text{Pyrr}], [\text{NTf}_2^-], [\text{OTf}], [\text{BF}_4^-], [\text{PF}_6^-]$	Higher IL extraction efficiencies of TH/DBT correlated to increased cation and anion surface area for absorption through van der Waals interactions. No significant IL-TH/DBT hydrogen bonding.	⁴⁵
2016, 2017	CAM-B3LYP/def2-SVP, BP86-D3/TZ2P(ZORA)//BP86/def2-SVP	$[\text{TBHEP}], [\text{TBCMP}], [\text{Br}]$	Hydrogen bonding between phosphonium ionic liquids (PILs) and TH/DBT/DMDBT combined with dispersion from cation alkyl chains were responsible for extraction efficiencies.	^{46, 47}

2.2. Ionic Liquid-Thiophenic Compound Complexation

Quantum mechanical investigations of IL-based EDS largely began with Lü et al. and focused on the ILs of $[\text{C}_4\text{MIM}][\text{BF}_4]$ / $[\text{C}_4\text{MIM}][\text{PF}_6]$ ³⁹ and $[\text{C}_1\text{MIM}][\text{MeSO}_4]$ ⁴⁰ treated with a DFT method that utilized the generalized gradient approximation (GGA) PW91 functional and the double numerical basis sets plus polarization functional (DNP). Despite PW91's difficulties treating dispersion,⁴⁸ the GGA/PW91/DNP method has been shown to be capable of describing interactions between conjugated systems.⁴⁹ Lü and coworkers later utilized the more advanced dispersion-corrected hybrid functional $\omega\text{B97X-D}$ in a follow up study of IL desulfurization using 1-butylypyridinium hydrogen sulfate $[\text{C}_4\text{Py}][\text{HSO}_4]$.⁴¹ Their reported methodology featured a “supermolecule” structure consisting of a single IL ion pair complexed to the target sulfur compound, e.g., TH, DBT, THO_2 , or DBTO_2 . These complexes were optimized over a range of configurations with ground states confirmed by frequency analysis. The systems were analyzed using Atoms in Molecules (AIM)⁵⁰ and Natural Bond Order (NBO)⁵¹ theories to examine the electron distribution present in these super structures. Their findings for the imidazolium-based ILs highlighted the importance of hydrogen bonding between the proton located on the highly Lewis-acidic C2 carbon that is flanked by both heterocyclic nitrogen atoms (Figure 2) and the fluorine and oxygen atoms of the respective counter anions BF_4 , PF_6 , and MeSO_4 . This electrostatic interaction was retained even during complexation with the refractory sulfur compounds. Consequently, strong adsorption of TH onto the ILs arose from 1) $([\text{C}_4\text{MIM}])\text{-H}\cdots\pi(\text{TH})$ hydrogen bonds, 2) $(\text{TH})\text{H}\cdots\text{F}([\text{PF}_6] \text{ or } [\text{BF}_4])$ hydrogen bonds, and 3) $\pi\cdots\pi$ stacking between the imidazolium ring and the thiophenic ring (Figure 3).³⁹ Similar findings were reported between $[\text{C}_1\text{MIM}][\text{MeSO}_4]$ and DBT, i.e., weak $\pi\cdots\pi$ interactions, $\text{C-H}\cdots\pi$ interactions, and hydrogen bonding.⁴⁰ Changing the IL cation to $[\text{C}_4\text{Py}]$ yielded many of the same favorable interactions for adsorption of TH and DBT with significant $\pi\cdots\pi$ stacking noted between the pyridinium ring and the thiophenic ring.⁴¹ While subsequent DFT-based

studies described below reflect many of these same general trends, particularly for imidazolium-based ILs, the importance of π - π stacking and hydrogen bond interactions in solubilizing TH and DBT has been questioned by others as communicated later in this section.

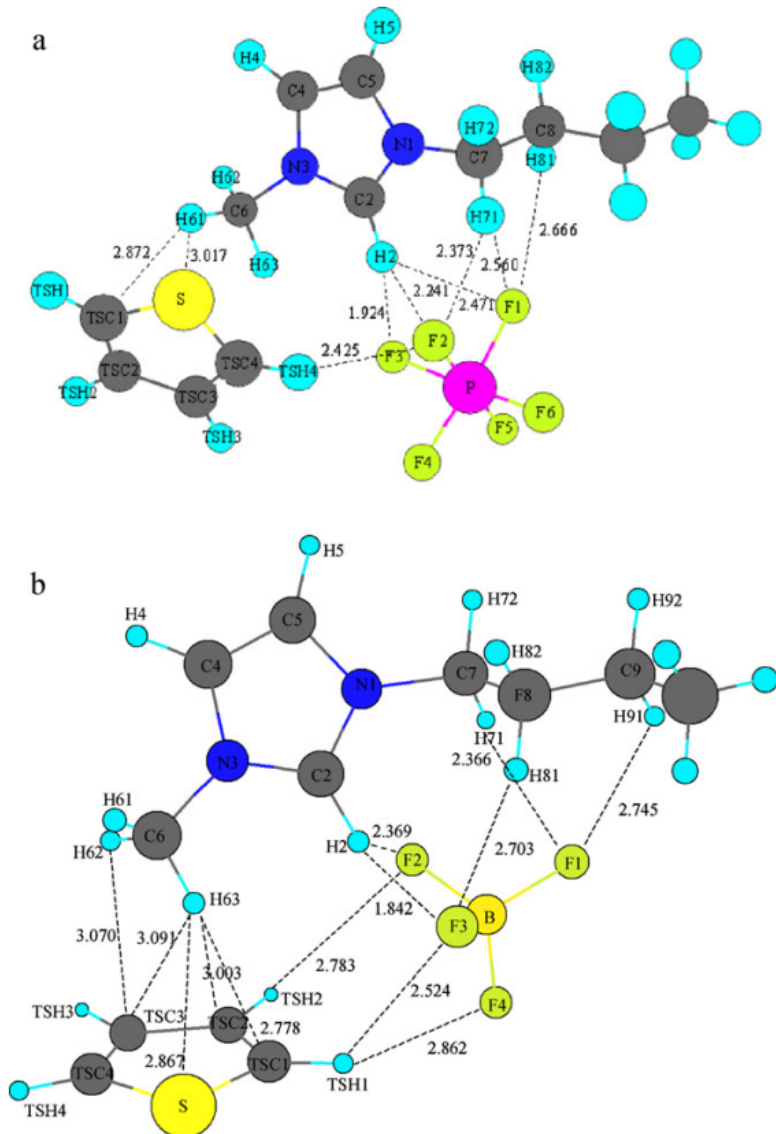


Figure 3. QM-derived geometrical configurations and atomic distances between TH and (a) [C₄MIM][PF₆] and (b) [C₄MIM][BF₄]. Reproduced with permission from ref. 39. Copyright 2012 Elsevier.

Li et al. computationally explored IL-driven EDS using the metal-containing IL $[\text{C}_4\text{MIM}][\text{AlCl}_4]$,⁴² a promising species utilized in Jess and coworkers' pioneering study.³³ In Li et al.'s work, an ion pair was complexed to a single refractory sulfur compound, i.e., TH, BT, or DBT (Figure 1), and computed using M06-2X in conjunction with an implicit solvent model developed by Truhlar and coworkers used to treat generic ionic liquids with the SMD model (SMD-GIL).⁵² Computed interaction energies between $[\text{C}_4\text{MIM}][\text{AlCl}_4]$ and the sulfur compounds followed the order of TH < BT < DBT. An energy decomposition analysis was performed using the block-localized wave function method (BLW-ED)⁵³ that revealed steric interactions (ΔE_s) dominated by accounting for approximately 55% of the interaction energy in the two systems examined, i.e., IL-TH and IL-BT. Polarization energy (ΔE_{pol}) and charge transfer (ΔE_{CT}) contributed approximately 25% and 18% of the interaction energy, respectively. Similar to results from Lü et al.'s earlier non-metal-containing IL-EDS computational studies,^{39, 40} the $[\text{C}_4\text{MIM}]$ cation contributed important π - π stacking with the aromatic rings of the sulfur compounds (TH/BT/DBT) while the $[\text{AlCl}_4]$ anion provided hydrogen bonding interactions. Interestingly, the $\text{CH}\cdots\pi$ interaction was not found to play a major role in this system. When using a high molar ratio of AlCl_3 , e.g., $[\text{C}_4\text{MIMCl}]:2[\text{AlCl}_3]$, an IL forms where $[\text{Al}_2\text{Cl}_7]$ is the dominant anion present instead of $[\text{AlCl}_4]$. Their calculation of a $[\text{C}_4\text{MIM}][\text{Al}_2\text{Cl}_7]$ -TH complex gave a weaker interaction energy compared to $[\text{C}_4\text{MIM}][\text{AlCl}_4]$ -TH suggesting that higher AlCl_3 molar ratios should not improve EDS performance. Accordingly, Zhang et al. reported experimentally that a trimethylammonium chloroaluminate (AlCl_3 -TMAC) IL composed with a high ratio of AlCl_3 was inferior for sulfur removal compared to a lower molar ratio.⁵⁴

In order to examine the effect of alkyl chain length in imidazolium-based ILs on desulfurization potential, Niknam et al. employed B3LYP to study the interactions between DBT and $[\text{C}_n\text{MIM}][\text{BF}_4]$ where $n = 2, 4, 6, 8$.⁴³ Their computed single ion pair and DBT

complexes found interaction energies became more favorable with increasing $[C_nMIM]$ alkyl chain length, which correlated with the experimental finding of Zhang et al. that showed preferential adsorption of DBT by $[C_nMIM][BF_4]$ for $n=4$ over $n=2$.⁵⁴ Dominant DBT- $[C_nMIM]$ π - π stacking and C-H \cdots π interactions were again computed and corroborated by NBO and AIM analyses, with the $[BF_4]$ anion taking up a complementary role. Their AIM analysis revealed the existence of 6-8 bond critical points (BCPs) that correlate to each hydrogen bond present in each system, with the number of BCPs increasing with increasing imidazolium alkyl chain length. As in the earlier computational DFT studies, they found the C2 proton of the $[C_nMIM]$ cation formed the strongest hydrogen bond directly with a fluorine atom of the $[BF_4]$ anion.

Investigation of imidazolium-based ILs and TH/DBT mixtures has also been extended to functionalized ILs. For example, Patra et al. reported a joint computational and experimental study examining EDS of TH/DBT using *ortho*-, *meta*-, and *para*-substituted nitrobenzyl groups in 3-benzyl-1-methylimidazolium bromide $[BzMIM][Br]$ ILs (Figure 2).⁴⁴ DFT calculations were performed on the ion pairs of $[o\text{-NO}_2BzMIM][Br]$, $[m\text{-NO}_2BzMIM][Br]$, and $[p\text{-NO}_2BzMIM][Br]$ in the gas-phase and in solution-phase using the integrated electric field polar continuum model (IEFPCM). IL-TH interactions were estimated implicitly by optimizing a single IL ion pair in a TH solution modeled using IEFPCM with the dielectric constant of TH (i.e., 2.7). Superior extraction performance was hypothesized to be a result of the electron-withdrawing nature of the NO_2 group that creates a more electron-poor imidazolium cation to bind with the electron-rich TH.⁴⁴ Their DFT calculations found an increasing free energy of solvation starting from 10.63 kcal/mol for the unsubstituted $[BzMIM]$ to 13.63, 14.75, and 15.69 kcal/mol for the *ortho*, *meta*, and *para* substituted cations, respectively. This trend was clearly reflected in the distance difference (Δd) between the imidazolium N and the Br anion in the gaseous and solution phase calculations, where computed Δd values of 0.02, 0.19, 0.22,

and 0.54 Å were found for the unsubstituted, *ortho*-, *meta*-, and *para*-substituted nitrobenzyl rings, respectively. From this observation, it was inferred that solvation of the IL was driven primarily by the developing positive charge at the N site which would presumably interact with the TH moiety. However, steric effects (i.e., the shielding of the imidazolium cation by nearby NO_2 groups) were calculated to be more influential than inductive effects in determining the solvation free energy with the exposed N site of [*p*-NO₂BzMIM] providing the most favorable binding environment for TH. While experiments performed generally agreed with their computational trends, the IEFPCM model used in place of an explicit TH molecule led to an overestimation of steric effects. Instead, experimental extraction efficiencies of DBT showed that [*m*-NO₂BzMIM], with its balance of strong inductive effect and low steric crowding of the imidazolium functional group, was the most efficient IL species.⁴⁴

Widening the scope to other heterocyclic nitrogen-based ILs, Player et al. investigated not only the well-studied [C_nMIM] (n = 2, 4, 6, 8, 10) and [C₄Py] cations, but also the 1-butyl-2,3-dimethylimidazolium [C₄C₁MIM] and 1-butyl-1methylpyrrolidinium [C₄C₁Pyrr] cations (Figure 2), bearing the bis-(trifluoromethylsulfonyl)imide [NTf₂], trifluoromethanesulfonate [OTf], [BF₄] and [PF₆] anions.⁴⁵ In this combined experimental and computational study, the AFPD method⁵⁵ was utilized due to its “dispersionless” DFT component, allowing dispersion interactions to be isolated and quantified. Individual cation-TH and anion-TH pairs were optimized separately in solution using a polarizable continuum model (PCM)⁵⁶ of 1-pentanol which has a dielectric constant of 15.1 that mimics the typical IL dielectric constant range of ~10-20.⁵⁷ Interestingly, their computational results suggested no significant hydrogen bonding exists between the IL anion and TH or DBT, with experimental extraction efficiencies better correlated to anion volume. In a similar fashion, increasing cation volume also positively correlated with increasing extraction efficiencies following the order of pyridinium > imidazolium > pyrrolidinium. Quantification of the dispersion contribution to both cation-TH

and anion-TH binding found a positive correlation between dispersion and total binding energies with an R^2 value of 0.964. Their findings suggest that higher extraction efficiency may be derived primarily from an increased ion surface area for absorption through van der Waals interactions with other factors, including interaction energies between the IL ions, anion shape, and C-H $\cdots\pi$ interactions from cation alkyl chains, contributing to a lesser extent.⁴⁵

Going beyond nitrogen-based heterocyclic cations, e.g., pyridinium, imidazolium, and pyrrolidinium, Azizian, Zolfigol, and coworkers explored the use of phosphonium ionic liquids (PILs) for the extraction of BT, DBT, and dimethyldibenzothiophene (DMDBT) from liquid fuel in a pair of papers.^{46,47} Their joint experimental and theoretical studies focused on the PILs of tri-*n*-butyl-(2-hydroxyethyl)phosphonium bromide, [TBHEP][Br],⁴⁶ and tributyl(carboxymethyl)phosphonium bromide, [TBCMP][Br].⁴⁷ These PILs were developed specifically for EDS to provide a species hydrophobic enough to be miscible with TH/DBT/DMDBT while ensuring immiscibility with petroleum components through the hydroxyethyl and carboxylic acid moieties in [TBHEP][Br] and [TBCMP][Br], respectively. Optimization of a [TBHEP]-DBT pair in the gas-phase using the DFT method CAM-B3LYP/def2-SVP yielded two dominant conformations, Type I and Type II, with energies within 0.5 kcal/mol of each other (Figure 4).⁴⁶ The Type I conformation featured a prominent hydrogen bond between the OH group on [TBHEP] and the S atom of DBT with NBO analysis confirming charge transfer occurring between the lone pair of the S-atom and the σ^* of the O-H. The Type II conformation found numerous weak interactions between the α -hydrogens of the methylene groups of [TBHEP] with both the π -system and S-atom in DBT. Similar conformations and the same value of interaction energy was computed for the gas-phase [TBCMP]-DBT pair.⁴⁷ Energy decomposition analysis using BP86-D3/TZ2P(ZORA)//BP86/def2-SVP confirmed that, in the Type I conformation, the σ -orbital interaction energy (ΔE_{disp}) between donor orbitals of DBT and s orbital of the hydroxy H atom

on the cation provided the main portion of the total interaction energy (ΔE_{int}). However, the Type II conformation dispersion interaction energy (ΔE_{disp}) was derived from multiple interactions between the α -hydrogens of the hydrocarbon chains on the cation and the π -system of DBT dominated for both the [TBHEP][Br]⁴⁶ and [TBCMP][Br]⁴⁷ PILs.

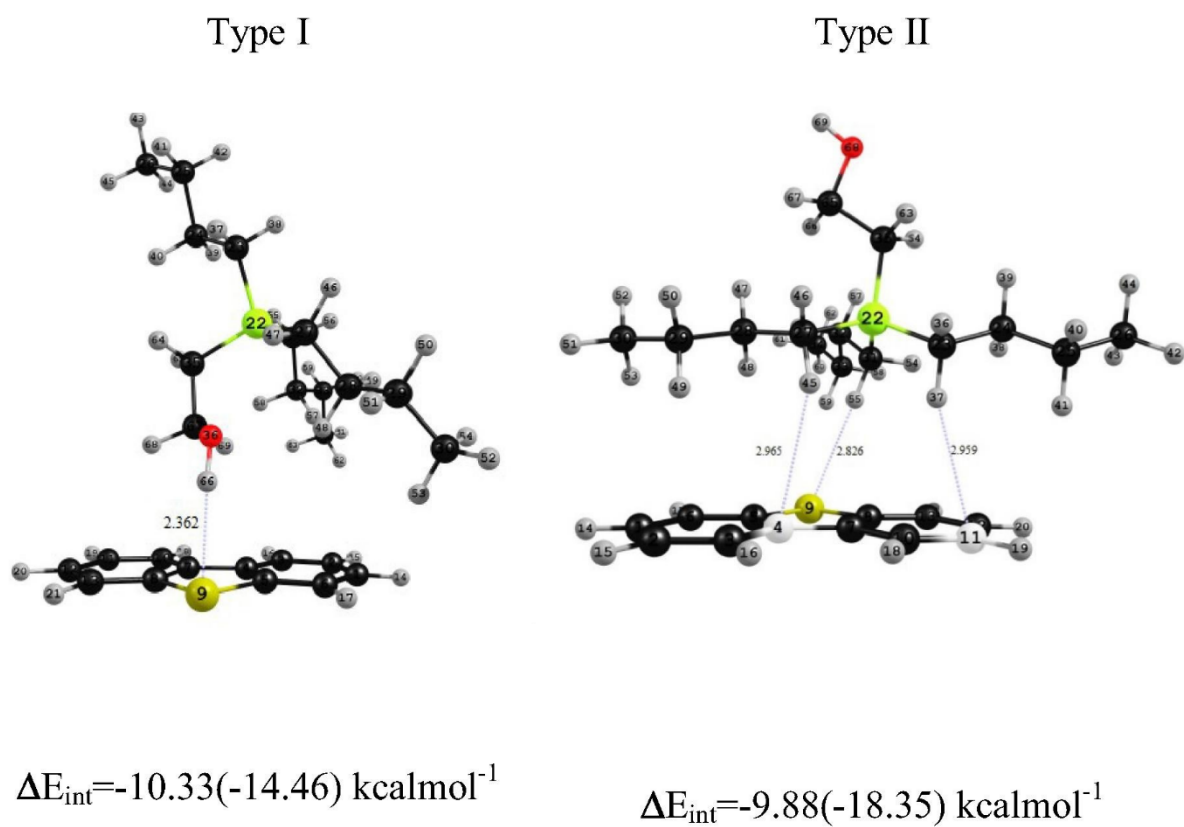


Figure 4. Optimized geometries of [TBHEP]-DBT dimers, showing the two dominant interaction forms present. Energy values are given using the CAM-B3LYP/def2-SVP level of theory with values in parenthesis obtained from BP86-D3/TZ2P(ZORA)//BP86/def2-SVP calculations. Reproduced with permission from ref. 46. Copyright 2017 Elsevier.

Table 3. Key Findings of Ionic Liquid Catalyzed Oxidation of Aromatic Sulfur Compounds to Analogical Sulfones Using Quantum Mechanical Calculations.

Year	QM Method	Ions Examined	Key Findings	Ref.
2015	B3LYP 6-31++G(d,p)	[MIM], [BF ₄]	Two transition states identified (DBT → DBTO and DBTO → DBTO ₂) with first oxidation as rate-limiting. Reduction in activation barrier attributed to IL hydrogen bonding that promoted H ₂ O ₂ cleavage. IL cation dominated DBTO ₂ extraction process.	⁵⁸
2016	B3LYP 6-31++G(d,p)	[C _n MIM] (<i>n</i> = 2, 4, 5, 6), [PF ₆]	Two transition states identified (TH → THO and THO → THO ₂) with first oxidation as rate-limiting. Increasing alkyl chain length in cation correlated to a reduction in the activation barrier	⁵⁹
2017	B3LYP B3LYP-D3 B2PLYPD 6-31++G(d,p)	[C ₄ MIM], [TFA]	Mechanism follows an initial oxidation of trifluoroacetate, [TFA], to CF ₃ COOO ⁻ by H ₂ O ₂ which then converts TH to THO ₂ . Cations and anions both play a major role during THO ₂ extraction.	⁶⁰

2.3. Ionic Liquids as Catalysts for Thiophenic Compound Oxidation

While the previous section showed that QM methods can be excellent tools for mapping intermolecular interactions between ILs and refractory sulfur compounds, their most prized utility lies in their ability to simulate chemical reactions, a feat that cannot be accomplished using classical simulations.⁶¹ In the context of fuel desulfurization, QM calculations can be employed to understand the catalytic role ILs play in the oxidation of TH/DBT to their analogical sulfones enabling a more facile extraction. Lo et al. established this concept in 2003 by combining ODS and EDS with ILs in their seminal work (Figure 5).⁶² They reported that the addition of H₂O₂/acetic acid as an oxidizing agent to [C₄MIM][BF₄] and [C₄MIM][PF₆] increased extraction efficiency of DBT from light oil by almost an order of magnitude over extraction with ILs alone. Subsequent work by Lu et al. reported similar efficiency improvements in the extraction of DBT using [C₆MIM][BF₄] and H₂O₂.⁶³ Changing the IL from imidazolium-based cations to pyridinium-based, e.g., [C₄Py],⁶⁴ and quaternary ammonium-based, e.g., [(C₄H₉)₄N],⁶⁵ cations also provided enhanced extraction of DBT from model oils and gasoline when using H₂O₂ emphasizing the potential for the discovery of even more effective ILs for oxidative-extractive desulfurization. Accordingly, the interest in using

ILs as a complementary process to ODS has continued to grow in the subsequent decades.^{9, 18, 66, 67} As the scientific community has steered their search for IL species that are extremely efficient in small volumes and highly recyclable, QM methodologies have provided a new avenue to pursue a more precise understanding of the catalytic mechanism underlying the oxidation of refractory sulfur compounds in this molten salt medium.

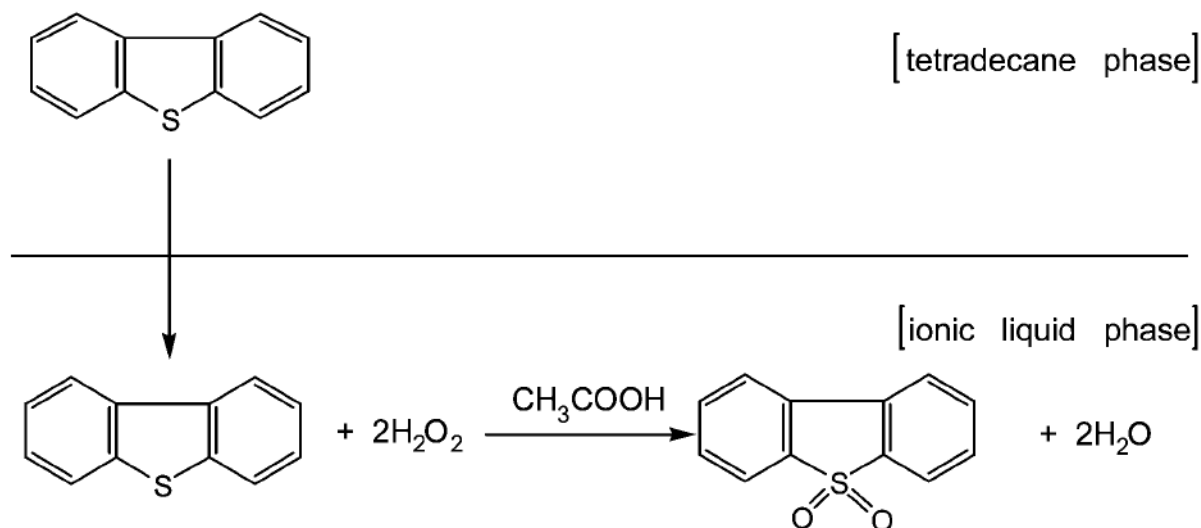
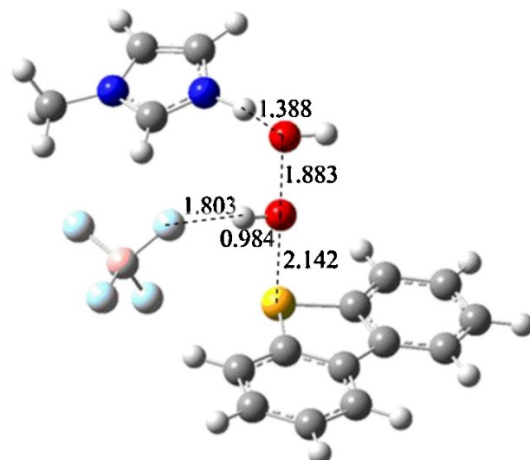


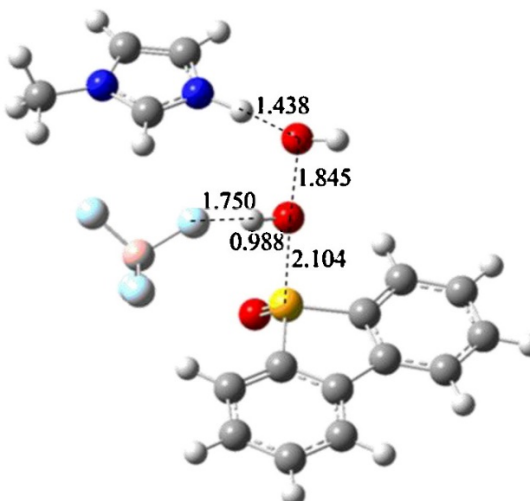
Figure 5. Scheme showing the phase-transfer and IL-mediated, peroxide-assisted oxidation of DBT to form its corresponding sulfone. Reproduced with permission from ref. 62. Copyright 2003 Royal Society of Chemistry.

A theoretical investigation into the IL-enhanced oxidation reaction of DBT into dibenzothiophene sulfone (DBTO₂) was carried out by Xu et al. to examine the origin of the catalytic effect provided by [MIM][BF₄], where [MIM] is 1-methylimidazolium.⁵⁸ They employed B3LYP to compute the energetics of the reaction pathway by using a super structure complex featuring a single [MIM][BF₄] ion pair, H₂O₂, and DBT. Invoking frontier molecular orbital (FMO) theory,⁶⁸ the authors found the oxidation of DBT by H₂O₂ proceeded via the

HOMO_{DBT} - $\text{LUMO}_{\text{H}_2\text{O}_2}$ interaction. The overall reaction mechanism was examined in detail and two transition states (TS1" and TS2") corresponding to $\text{DBT} \rightarrow \text{DBTO}$ and $\text{DBTO} \rightarrow \text{DBTO}_2$, respectively, were confirmed using intrinsic reaction coordinate (IRC) calculations (Figure 6). The TS1" and TS2" activation barrier energies were computed to be 13.1 and 23.8 kcal/mol, respectively, in the presence of $[\text{MIM}][\text{BF}_4]$, whereas the uncatalyzed reaction gave much larger values of 32.1 and 37.0 kcal/mol; energy barriers were reported relative to intermediate structures leading to the TS and not separated reactants. The significant barrier reduction in the IL was attributed to two important hydrogen bonds that promoted O-O and O-H cleavage of H_2O_2 . The first of these interactions involved $[\text{BF}_4]\text{-H}_2\text{O}_2$ with an O-H \cdots F hydrogen bond between fluorine and the proton bound to the nucleophilic oxygen attacking DBT. Simultaneously, the other interaction entailed $[\text{MIM}]\text{-H}_2\text{O}_2$ with the proton bound to the imidazolium nitrogen atom hydrogen bonding with the second peroxide oxygen, N3-H \cdots O (Figure 6). The authors also examined the role of $[\text{MIM}][\text{BF}_4]$ in the extraction of DBT and DBTO_2 using B3LYP-optimized complexes. Stronger binding of the IL with DBTO_2 was computed (-11.9 kcal/mol) when compared to DBT (-6.6 kcal/mol) which may be expected given the larger calculated dipole of 5.77 D for DBTO_2 compared to 0.78 D for DBT. Interestingly, calculation of individual $[\text{MIM}]\text{-DBTO}_2$ and $[\text{BF}_4]\text{-DBTO}_2$ pairs found the interaction energy involving the cation to be much stronger at -26.1 kcal/mol compared to the -16.1 kcal/mol with the anion. This may suggest that the cation plays a more important role during the extraction and separation process.⁵⁸



TS1'' (399i)



TS2'' (354i)

Figure 6. Optimized B3LYP geometries of the transition states of DBT \rightarrow DBTO and DBTO \rightarrow DBTO₂ with H₂O₂ in [MIM][BF₄]. Distances given in angstroms and values in parenthesis denote the imaginary frequencies. Reproduced with permission from ref. 58. Copyright 2015 Elsevier.

Yuan et al. investigated the effect of alkyl chain length in the oxidation of TH to sulfone (THO₂) by examining ILs composed of the [C_nMIM] (n = 2, 4, 5, 6) cations and the [PF₆] anion.⁵⁹ In their work, B3LYP was used to compute the energetics of the reaction pathway with

a supermolecule complex of a single IL ion pair, H₂O₂, and TH. The complete reaction pathway was computed and as expected two transition states (TS1 and TS2) were located that corresponded to the transformations of TH → sulfoxide (THO) and THO → THO₂, respectively. The authors determined the first oxidation step (TS1) to be rate-limiting, similar to Xu et al.'s study where the first oxidation step of DBT → DBTO in [MIM][BF₄] had the highest absolute energy.⁵⁸ Yuan et al. found that increasing the length of the alkyl chain correlated with a reduced activation barrier, i.e., the ethyl, butyl, amyl, and hexyl side chains gave activation barriers of 27.6, 26.5, 23.4, and 21.3 kcal/mol, respectively.⁵⁹ Nevertheless, all ILs significantly lowered the uncatalyzed reaction energy of 80.5 kcal/mol. Their NBO analysis showed the electron density on the TH sulfur was influenced by the alkyl side chain length with the positive charge on the S atom increasing from 0.462, 0.479, 0.483, and 0.485 e for the ethyl, butyl, amyl, and hexyl based ILs, making it more susceptible to oxidation via H₂O₂. Little effect on the charge of the nucleophilic O atom in H₂O₂ was found with changing alkyl length. Similar to Xu et al.'s reported interactions between DBT/DBTO₂ and [MIM][BF₄],⁵⁸ Yuan et al. found the cations to have a greater binding affinity with TH/THO₂ than the anions and ion pairs. Interestingly, NBO analysis determined that the cation-TH/THO₂ binding energies slightly decreased with increasing alkyl chain length during the extraction process.⁵⁹

Further computational examination of the IL-catalyzed oxidative-extractive mechanism was carried out by Wang et al. for the oxidation of TH to THO₂ in an IL composed of [C₄MIM] and trifluoroacetate, [TFA], using H₂O₂ as the oxidant.⁶⁰ The B3LYP method was used to optimize various superstructure complexes composed of different combinations of ions, oxidant, and TH. Single-point calculations were then computed using B3LYP-D3 on the frequency-confirmed stationary points to provide dispersion corrections⁶⁹ to the final energies. Two potential mechanisms were explored where 1) [TFA] is first oxidized to the peracid CF₃COOO⁻ by H₂O₂ which then converts TH to THO₂, or 2) TH is directly oxidized by H₂O₂.

with the IL acting as a spectator. The first mechanism gave the lowest activation barrier of 36.8 kcal/mol for the rate-limiting transition state involving peracid formation. In the second mechanism, a three-molecule transition state complex of a [C₄MIM][TFA] ion pair, H₂O₂, and TH gave a higher activation energy of 38.3 kcal/mol. In terms of extractive ability of the IL, the [C₄MIM] and [TFA] ions showed stronger interactions with THO₂ than TH as expected. Interestingly the cation-THO₂ and anion-THO₂ pairs themselves gave similar interaction energies of -16.7 and -17.0 kcal/mol, respectively, indicating that both ions play a major role during extraction.

2.4. IL-EDS Design Implications Derived from QM Calculations

Multiple DFT studies in Section 2.2 emphasized the outsized role played by π - π stacking, C-H \cdots π interactions, and hydrogen bonding between the *N*-heterocyclic IL ions and the refractory sulfur compounds in the IL-driven EDS process.^{39-41, 43} In the case of imidazolium-based ILs, particularly strong hydrogen bonding was noted between the proton located on the C2 atom (Figure 2) and the anion, even in the presence of TH/DBT. Alkyl chain length in [C_nMIM] also affected the solubilization of the sulfur compounds as increasing chain length was correlated to enhanced interaction energies, mirroring experimental results that showed a more efficient extraction of DBT by [C_nMIM][BF₄] for $n=4$ over $n=2$.⁵⁴ Quantification of dispersion effects on TH extraction was investigated more thoroughly by Player et al. with a positive correlation found between dispersion and total binding energies.⁴⁵ Their work suggested higher extraction efficiency may be derived primarily from an increased ion surface area for absorption.⁴⁵ To that end, alternative heterocycles bearing a larger aromatic core, such as pyridinium derivatives,^{41, 45} provided another viable route to improve dispersion interactions with TH/DBT. Patra et al. functionalized imidazolium-based ILs with nitrobenzyl groups to develop greater positive charge at the N site for improved TH interaction.⁴⁴ Surprisingly, steric effects (i.e., the shielding of the imidazolium cation by nearby NO₂ groups)

were calculated to be more influential than inductive effects.⁴⁴ The impact of the IL anionic components have been less thoroughly studied computationally; however, most common ions, e.g., $[\text{BF}_4^-]$, $[\text{PF}_6^-]$, $[\text{AlCl}_4^-]$ and $[\text{MeSO}_4^-]$, exhibited similar hydrogen bonding interactions with TH/DBT despite changes in the IL cation. Player et al. did perform a more systematic study on anion effects and concluded that anions with larger volumes provided a moderate beneficial impact in extraction efficiency.⁴⁵

The use of ILs as both catalysts and extractants in a combined ODS-EDS process is also ripe for exploration by using DFT methodology to energetically map entire reaction pathways. For example, the oxidation mechanisms of TH to THO_2 and DBT to DBTO_2 were computationally examined using H_2O_2 as the oxidant in ILs composed of $[\text{C}_n\text{MIM}]$ with $[\text{BF}_4^-]$ or $[\text{PF}_6^-]$.^{58, 59} Significant barrier reductions in ILs were attributed to important hydrogen bonds provided by the IL ions to H_2O_2 at the transitions state that promoted O-O and O-H cleavage when reacting with the refractory sulfur compounds. Yuan et al. found that increasing the length of the alkyl chain in $[\text{C}_n\text{MIM}]$ correlated with a reduction in the activation barrier through weak hydrogen bonding interactions that modulated the electron density of the TH sulfur atom making it more susceptible to oxidation.⁵⁹ New catalytic pathways were also explored by using a $[\text{TFA}]$ anion that reacted with H_2O_2 to form CH_3COO^- that directly oxidized TH to THO_2 .⁶⁰ The DFT calculations found the formation of the peracid to be rate-limiting, so the IL itself was participating in the reaction rather than acting as a spectator. This highlights the ability of DFT to explore additional oxidants for improved oxidation efficiency in future work.

2.5. QM Methodology Recommendations

The QM method selected is of the upmost importance for reproducing and predicting the subtle interplays of sterics, dispersion interactions, and hydrogen bonding present between

the ILs and refractory sulfur compounds. To that end, the use of DFT hybrid functionals, e.g., B3LYP, M06-2X, and ω B97X-D, have been shown to provide the best compromise between accuracy and efficiency for ionic liquid clusters.⁷⁰ Frequently reported in the IL-driven EDS studies was the presence of significant non-covalent interactions in the form of π - π stacking and C-H \cdots π interactions. However, traditional DFT, e.g., GGA, often fail to account for dispersion forces as electron correlation effects are not adequately captured. Several of the studies discussed here incorporated dispersion effects into DFT calculations through different approaches that included empirical dispersion corrections (DFT-D3), non-local van der Waals functionals (vdW-DF), and hybrid functionals that contain a portion of exact exchange from Hartree-Fock theory.^{70, 71} Another important consideration is the choice of basis set to approximate the electronic wavefunctions. Diffuse functions are absolutely necessary to properly describe the IL anionic species and extending diffuse functions to hydrogen atoms helped to better evaluate hydrogen bonding strength.⁷² Most studies highlighted in this minireview employed larger triple-zeta basis sets, where the forms of 6-311++G(d,p) and cc-pVTZ can be recommended to handle the complexities of the IL solvents.⁷⁰ Incorporation of bulk solvent effects were typically handled using an implicit solvent model, e.g., PCM⁵⁶ and SMD-GIL,⁵² that treated the solvent as a continuous medium characterized by its dielectric constant. While this provides a reduction in computational cost compared to the thousands of explicit solvent molecules commonly used in molecular dynamics simulations, in some cases explicit molecules are needed. For example, Patra et al. showed the IEFPCM model used in place of an explicit TH molecule led to an overestimation of steric effects.⁴⁴ Finally, AIM⁵⁰ and NBO⁵¹ proved to be powerful tools for detailed examination of the electron distribution present in these complex structures composed of ions, sulfur compounds, and, in the case of ODS, oxidants.

3. Molecular Dynamics (MD) Simulations

3.1. MD Introduction

While QM optimizations of IL ion pairs have provided considerable insight into the nature of the intermolecular interactions driving EDS and the chemical reactions occurring during ODS, the high computational cost of these methods prohibits scaling towards larger bulk solvent-sized systems. As an alternative, molecular dynamics (MD) simulations can readily compute the physical movement of thousands to tens of thousands of atoms on modest computer resources, thereby providing an excellent method for deriving detailed insight into the structure, dynamics, and thermodynamics of the molten salt environment. In addition, MD simulations can be used to examine various physical properties of ILs important for desulfurization, including viscosity, diffusivity, and density. MD methodology deviates quite considerably from QM, as electrons are not considered explicitly in the form of a wavefunction. Instead, the interactions between particles are described using a potential energy function, i.e., a “force field” featuring equations capable of describing both bonded (bond stretching, angle bending, and torsion rotation) and non-bonded (van der Waals and electrostatic) interactions present between atoms.⁷³ As such, the reliability of MD simulations is heavily dependent upon the accuracy of the force field used to describe the ILs of interest.⁷⁴ An additional challenge in simulating these complex systems is ensuring the proper sampling of relevant configuration space to match the experimentally measured ensemble average.⁷⁵ This section provides further insight into the desulfurization process through MD studies that aimed to replicate the explicit solvation of refractory sulfur compounds with hundreds of IL ion pairs (a summary is provided in Table 4). Developmental improvements of these models are also briefly discussed in the context of ILs and EDS simulations.

Table 4. Key Findings of Ionic Liquid-Mediated Extractive Desulfurization Derived from Molecular Dynamics Simulations.

Year	Force Field	ILs Examined	Key Findings	Ref.
2010	AMBER	$[\text{C}_n\text{MIM}]$ ($n = 4, 6, 8, 10$), $[\text{PF}_6]$, $[\text{BF}_4]$	Simulations of 256 IL ion pairs with DBT & DBTO_2 found an inverse correlation where the weaker the (anion)-F \cdots H- $[\text{C}_n\text{MIM}]$ hydrogen bond, the stronger the (DBTO_2) -O \cdots H- $[\text{C}_n\text{MIM}]$ hydrogen bond. Contradicts previous suggestion that larger anion volumes are responsible for improved desulfurization. Also found inclusion of water improved extractive desulfurization.	⁷⁶
2016	OPLS	$[\text{C}_4\text{MIM}]$, $[\text{BF}_4]$	Simulations of 250 IL ion pairs with 34 TH molecules found the TH to preferentially π - π stack with the cation ring rather than interact with the alkyl chains. Equilibrium solubility of TH was estimated to be 45 times larger than in <i>n</i> -dodecane.	⁷⁷
2017	AMBER	$[\text{C}_n\text{MIM}]$ ($n = 2, 4, 6, 8$), $[\text{PF}_6]$, $[\text{BF}_4]$	Simulations of 256 IL ion pairs with 9 DBT or DBTO_2 were used to compute the fractional free volume (FFV) to determine the distribution of sulfur compounds in ILs. Shorter cation alkyl chains ($n = 2, 4$) displayed DBT aggregation whereas longer chains ($n = 8$) gave good DBT dispersion that promoted more facile extraction.	⁷⁸
2021	OPLS	$[\text{C}_4\text{MIM}]$, $[\text{BF}_4]$, $[\text{Cl}]$, $[\text{Br}]$, $[\text{CH}_3\text{COO}]$	Simulations of 400 IL ion pairs with TH were used to calculate excess chemical potentials to predict $[\text{CH}_3\text{COO}]$ as the ideal anion for desulfurization. Stronger electrostatic/dispersion interactions were present between TH and the anions rather than cations.	⁷⁹
2023	OPLS	$[\text{C}_4\text{MIM}]$, $[\text{PF}_6]$, $[\text{BF}_4]$, $[\text{Cl}]$, $[\text{SCN}]$, $[\text{NTf}_2]$	Simulations of 500 IL ion pairs with TH, DBT, and MDBT were used to calculate excess chemical potentials to predict $[\text{NTf}_2]$ as the ideal anion for desulfurization. Stronger electrostatic/dispersion interactions were present between TH and the anions rather than cations. Two IL analogues (deep eutectic solvents) were found to have reduced extraction efficiency compared to ILs.	⁸⁰
2018	OPLS	$[\text{C}_n\text{MIM}]$ ($n = 2, 4$), $[\text{BF}_4]$, $[\text{SCN}]$	Simulations where half of the periodic box contained 350 dodecane molecules and the other half contained 400-500 IL ion pairs examined the phase-transfer behavior of TH & DBT. Smaller cation ($n=2$) had tighter π - π interactions making it less efficient for TH/DBT absorption from the oil phase into IL compared to the larger cation ($n=4$).	⁸¹
2020	AMBER	$[\text{AMPy}]$, $[\text{C}_2\text{MPy}]$, $[\text{C}(\text{CN})_3]$	Simulation of a complex fuel model with IL and TH found the allylic chain in $[\text{AMPy}]$ provided improved π - π stacking and stronger interaction energies compared to ethyl group in $[\text{C}_2\text{MPy}]$.	⁸²
2021	OPLS, UFF, AMBER	$[\text{C}_n\text{MIM}]$ ($n = 2, 4, 6$), $[\text{FeCl}_4]$	Simulation of magnetic ILs, <i>n</i> -dodecane, and DBT found strong interactions between S-atom of DBT and IL cations, but reduced interaction with the anion. No evidence of parallel π - π stacking between cation and DBT.	⁸³

3.2. Modeling Desulfurization in Bulk IL Environments

The earliest reported MD simulations of IL-mediated EDS was published in 2010 by Liu et al. when they examined systems composed of $[C_nMIM][PF_6]$ ($n = 4, 6, 8$, and 10) and $[C_{10}MIM][BF_4]$ with DBT and $DBTO_2$.⁷⁶ The AMBER force field formalism⁸⁴ was used with custom DBT/ $DBTO_2$ parameters developed by Liu et al.⁷⁶ and IL force field parameters obtained from work reported in 2004 by a different Liu et al. research team.⁸⁵ A significant advantage for MD over the earlier QM calculations, is the ability to analyze the effect of several factors upon desulfurization including varying the amounts of sulfur and water content and using different operating temperatures (300 and 343 K). Each simulation generally consisted of 256 IL ion pairs, 70-90 H_2O molecules (if water was included), and 9 DBT or 2-20 $DBTO_2$. Interactions between the ILs and DBT/ $DBTO_2$ were analyzed using radial distribution functions (RDFs), which provide the average distribution of particles around a central reference particle. The RDF analysis found the protons directly attached to the $[C_nMIM]$ ring gave very weak interactions with the S atom of DBT and instead preferred to interact with F atoms on the anions, similar to findings reported in multiple DFT-based studies.^{39-41, 43} However, significant hydrogen bonding did occur between some of the imidazolium ring protons and the O atoms of $DBTO_2$, particularly for the cations with the longest alkyl chain lengths, i.e., $[C_nMIM]$ where $n = 8$ and 10 . This is consistent with Bösmann et al.'s experimental study that emphasized the importance of cation size upon extraction.³³ In addition, the MD simulations found that adding small amounts of water provided positive effects on the extractive desulfurization ability of the more hydrophilic ILs, such as $[C_{10}MIM][BF_4]$. Finally, examination of the anions found $[BF_4]$ to have more negatively charged fluorine atoms than $[PF_6]$. This led to an inverse correlation where the weaker the $F\cdots H-[C_{10}MIM]$ hydrogen bond, the stronger the $(DBTO_2)\cdots O\cdots H-[C_{10}MIM]$ hydrogen bond leading to improved desulfurization for $[PF_6]$ over $[BF_4]$. This

provided an alternative hypothesis to the suggestion by Player et al. that larger anion volumes are primarily responsible for improved desulfurization efficiency.⁴⁵

Oliveira et al. performed MD simulations six years later on an IL system composed of [C₄MIM][BF₄] with TH and found π - π stacking between the imidazolium ring and the thiophenic ring to dominate over C \cdots π interaction with the alkyl chain.⁷⁷ This agrees with experimental observations regarding the importance of aromatic π interactions in desulfurization efficiency³⁴ and suggests that the IL alkyl chains primarily interact with hydrophobic molecules present in petroleum streams. However, beyond solute-solvent interactions, another major consideration in desulfurization performance is the available free volume in ILs for packing refractory sulfur compounds. To examine this concept, Cheng et al. performed MD simulations of [C_nMIM][BF₄] ($n = 2, 4, 6, 8$) and [C₈MIM][PF₆] with DBT and DBTO₂.⁷⁸ The fractional free volume (FFV) was calculated to determine the distribution of sulfur compounds in the ILs. The MD simulations were performed with 256 IL ion pairs and 9 solutes using the GROMACS software⁸⁶ and with the same force field parameters used in the earlier study by Liu et al.^{76, 85} The dispersion of DBT in ILs was studied by using RDF analysis between the center-of-mass of two DBT molecules. In ILs with shorter alkyl chains, i.e., [C_nMIM][BF₄] with $n = 2$ and 4, the RDFs displayed significant aggregation of the DBT molecules, whereas with increasing alkyl chains, $n = 8$, the RDF distanced increased considerably indicating good dispersion of DBT in the ILs. Accordingly, computed coordination numbers between ILs and DBT were lower for the longer alkyl chain ILs, which is indicative of greater dispersion within the solvent. Overall, increasing FFV correlated with more efficient packing of the sulfur compounds into the IL cation-anion network promoting more facile extraction from fuel.

Infinite dilution activity coefficient (γ_i^∞) measurements describe the thermodynamic nonideality between two substances that arise exclusively from solute-solvent intermolecular interactions and have been shown to be useful for vetting ILs as S-extractants.⁸⁷ As such, excess chemical potentials values ($\mu_i^{ex,\infty}$), which can be derived from (γ_i^∞), were computed by Verlarde-Salcedo et al. for TH in four ILs composed of the [C₄MIM] and the [Cl], [Br], [BF₄], and acetate [CH₃COO] anions.⁷⁹ In their work, the excess Gibbs free energy was computed by transferring one TH molecule into an IL box using free energy perturbation MD (or FEP-MD) simulations at temperatures of 300 and 343.14 K. The FEP-MD simulations were carried out with the GROMACS software⁸⁶ and the ILs were modeled using the accurate OPLS-VSIL force field developed by Doherty et al.⁸⁸ Verlarde-Salcedo et al. reported the [BF₄]- and [CH₃COO]-based ILs gave the most favorable $\mu_i^{ex,\infty}$ values suggesting their potential in sulfur extraction.⁷⁹ Yue and Acevedo expanded upon their work, by computing $\mu_i^{ex,\infty}$ values using the same FEP-MD methodology for systems comprised of TH, DBT, and 4-methyldibenzothiophene (MDBT) in ILs composed of [C₄MIM] with [Cl], [SCN], [BF₄], [PF₆], and [NTf₂] anions.⁸⁰ Two ionic liquid analogues, namely the deep eutectic solvents (DESs)⁸⁹ ethaline and glyceline, were also examined.⁸⁰ Yue and Acevedo found the [C₄MIM][NTf₂] IL to yield the best $\mu_i^{ex,\infty}$ values for all refractory sulfur compounds examined, with a trend correlating more favorable $\mu_i^{ex,\infty}$ energy to increasing anion size. The same observed trend was reported experimentally by Player et al. for S-extraction efficiency of TH and DBT where [NTf₂] > [PF₆] > [BF₄] in [C₄MIM]-based ILs.⁴⁵ Yue and Acevedo also reported the computed excess chemical potentials predicted a reduced desulfurization potential for DESs compared to the ILs.⁸⁰ Interestingly, structural analyses of their respective MD simulations by both Verlarde-Salcedo et al.⁷⁹ and Yue and Acevedo⁸⁰ found stronger electrostatic/dispersion interactions present between TH and the anions rather than cations. Noteworthy hydrogen bonding between the C2 proton on the imidazolium ring (Figure 2) and

S from TH/DBT/MDBT was found in ILs with larger anions, i.e., $[\text{PF}_6^-]$ and $[\text{NTf}_2^-]$, following the same trend discussed earlier by Liu et al. of weakened interactions between ions leading to stronger interactions with the DBT/DBTO₂ compounds.⁷⁶

To examine the phase-transfer behavior of thiophenic compounds at the IL-oil interface, Singh et al.⁸¹ constructed simulation boxes where half of the periodic box contained 350 dodecane molecules (oil model) and the other half contained 400-500 ion pairs of one of four unique ionic liquids, i.e., $[\text{C}_n\text{MIM}]^+[\text{BF}_4^-]$ or $[\text{C}_n\text{MIM}]^+[\text{SCN}^-]$, where $n = 2$ or 4. TH or DBT were inserted into the dodecane side of this biphasic system and MD simulations using GROMACS⁸⁶ were performed to examine their diffusion and adsorption to the dodecane-IL interface and into the bulk IL phase (Figure 7). Adsorption of the incoming sulfur compound was more pronounced in the IL with the larger cation, $[\text{C}_4\text{MIM}]^+$, regardless of the anion used, which again confirmed the findings of previous QM and MD studies of more facile sulfur extraction with increased cation size. Singh et al. computed diffusion coefficients to be ~ 2 -fold higher for DBT than TH in migrating from the bulk dodecane phase to the interface of dodecane-IL. The authors hypothesized that higher diffusion coefficients should correlate to higher rates of extraction. Interestingly, in pure ILs the trend reverses where DBT diffuses slower than TH indicative of strong intermolecular interactions between DBT and ILs alongside a higher mass density for DBT that makes it bulkier to move in the IL relative to TH. Examination of TH/DBT-solvent interactions at the oil-IL interface showed favorable π - π stacking and C-H \cdots π interactions as the driving force for phase transfer to the IL from dodecane.

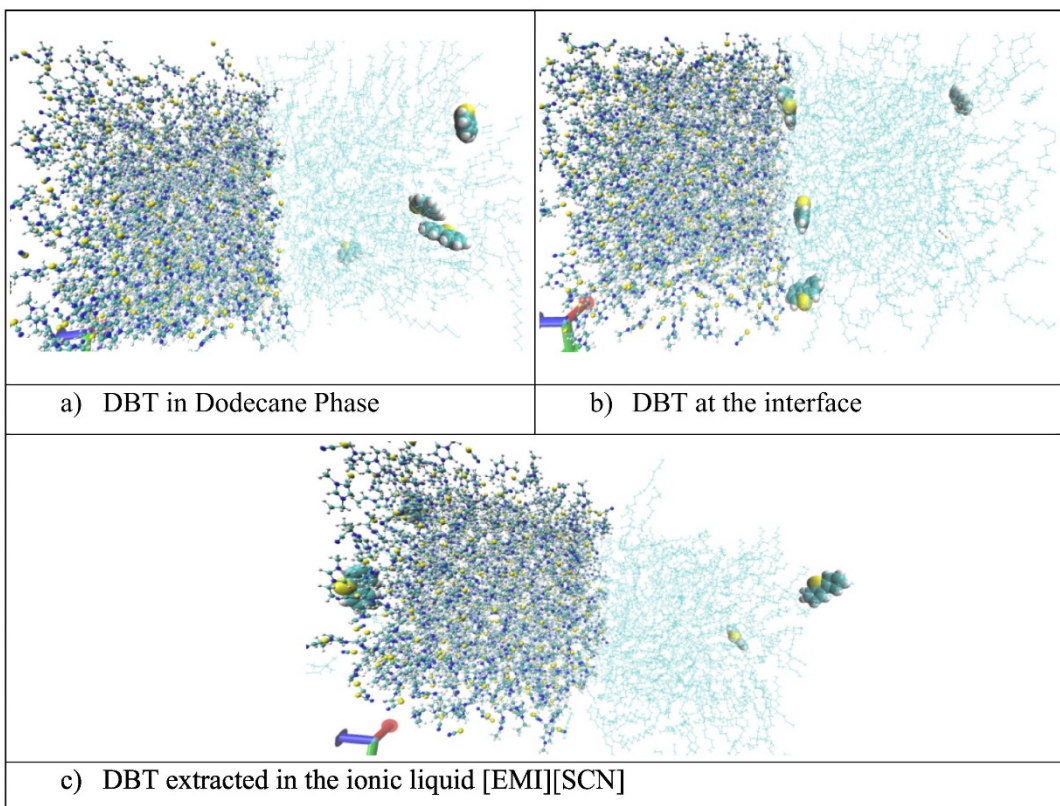


Figure 7. Representative snapshots from MD simulations of DBT in a biphasic model of dodecane and $[\text{C}_2\text{MIM}][\text{SCN}]$. Reproduced with permission from ref. 81. Copyright 2018 Elsevier.

Wang et al. used computer-aided IL design (CAILD) to identify and examine a class of pyridinium cations with a methyl group *ortho* to the nitrogen atom [MPy] and various functional groups attached directly to the nitrogen atom (e.g., hydroxyl, methoxy, vinyl, cyanomethyl).⁸² Of the top candidates identified for EDS, MD simulations were performed on ILs composed of the aforementioned cation with an allylic or ethyl functional group attached to nitrogen, [AMPy] (Figure 2) and $[\text{C}_2\text{MPy}]$, respectively, and a tricyanomethanide anion, $[\text{C}(\text{CN})_3]$. The authors simulated model fuel-IL systems composed of 306 *n*-octanes, 81 toluenes, 89 cyclohexanes, 6 TH, and 222 $[\text{AMPy}][\text{C}(\text{CN})_3]$ or 234 $[\text{C}_2\text{MPy}][\text{C}(\text{CN})_3]$ ion pairs. The GROMACS software⁸⁶ was used for the MD simulations with AMBER force field⁸⁴

parameters. RDF analysis of both ILs systems found a general pattern of the $[\text{C}(\text{CN})_3]$ anion surrounding the H atoms of TH, while the $[\text{MPy}]$ cation formed π - π stacking interactions with TH. However, the major difference between the ILs was that the allylic group in $[\text{AMPy}]$ promoted a much closer distribution of the IL around TH in comparison to $[\text{C}_2\text{MPy}]$. For example, the RDFs between S of TH and the terminal C atoms on the sidechain exhibited a closer first peak of 3.69 Å for the allylic group versus 3.93 Å for the ethyl group. Energy analysis revealed that while the $[\text{C}(\text{CN})_3]$ anion exhibited similar interaction energies in both ILs, the allylic substitution gave a lower interaction energy by \sim 1.1 kcal/mol indicative of stronger interactions with TH compared to the ethyl substituted cation. Finally, RDF analysis of the $[\text{MPy}]$ -based ILs with the other various fuel components revealed that weaker interactions were present between the cations and the non-thiophenic fuel components, emphasizing the preferential solvation of TH by the molten salts.

A major issue after EDS completion is the costly separation of the extraction solvent. An innovative solution for enabling a more effective separation is the use of magnetic ionic liquids (MILs) that combine the advantages of traditional ILs with the unique ability to respond to magnetic fields.⁹⁰ DFT-based studies using MILs for TH/DBT extraction have been reported by Ko et al.,⁹¹ Martínez-Magadán et al.,⁹² and Li et al.⁹³ with a major focus on $[\text{C}_4\text{MIM}][\text{FeCl}_4]$.⁹⁴ Their DFT studies emphasized the interaction between TH/DBT and $[\text{FeCl}_4]$ with the mechanism of extraction attributed several factors, such as donation and back-donation mechanisms⁹² or charge transfer effects.⁹³ Examination of MILs using MD simulations have been more limited owing to a lack of well-developed force field parameters.⁹⁰ However, Daneshvar et al.⁸³ reported an MD study of $[\text{C}_n\text{MIM}][\text{FeCl}_4]$ ($n = 2, 4, 6$) with DBT and *n*-dodecane, where mixed force field parameters were assembled using Moltemplate, a cross-platform molecule builder for LAMMPs.^{95, 96} The MD simulations found the $[\text{C}_4\text{MIM}][\text{FeCl}_4]$ IL to yield the best desulfurization percentage and a positive correlation was

reported between improved extraction efficiency and both increasing temperature and increasing IL loading. Domain analysis showed complete dispersion of DBT in the IL with a strong association between the S-atom of DBT and the imidazolium cations. Surprisingly, no evidence of parallel π - π stacking was found in stark contrast to the multiple MD and QM studies of non-metal ILs discussed earlier. A major limitation of the current MD simulations is their inability to investigate the donation and back-donation mechanisms⁹² and charge transfer effects⁹³ observed in the QM studies between sulfur compounds and $[\text{FeCl}_4]$ due to the use of a fixed-charge force field.⁷³ Future MIL-mediated EDS simulations studies may consider the use of a polarizable force field⁷⁴ or ab initio molecular dynamics to capture these effects (see the “Future Directions” section).

3.3. IL-EDS Design Implications Derived from MD Simulations

QM calculations (Section 2) have provided unparalleled accuracy in the description of important interactions present in isolated complexes, e.g., π - π stacking and $\text{CH}\cdots\pi$ between cations and sulfur compounds. While MD simulations confirmed their prevalence,⁷⁷ they have also highlighted the necessity of bulk solvent to be considered in the desulfurization process. For example, the role that anions play in EDS were given secondary consideration in most QM studies as they often yielded weaker interaction energies with the sulfur compounds compared to the cations.^{39-41, 43} Yet, MD studies determined that the choice of anion had a marked effect on the packing and geometrical arrangements of the incoming sulfur compounds,^{78, 81} diffusion coefficients,⁸¹ excess chemical potential,^{79, 80} and hydrogen bonding between the cation and sulfur compounds.^{76, 80} The experimentally observed correlation between IL ion size and sulfur extraction efficiency³³ was attributed to dispersion and ion surface absorption from QM studies;⁴⁵ however, MD simulations by several research groups have provided an alternative explanation that found weaker interactions between the cations and larger anions led to stronger hydrogen bonding between the cations and refractory sulfur compounds.^{75, 79, 80} Beyond the

QM-emphasized electrostatic interactions, MD simulations by Cheng et al. have also shown a positive correlation between available free volume in the ILs and EDS efficiency, where increasing alkyl chain length in $[C_nMIM]$ created lower-density ILs that disrupted aggregation of the refractory sulfur compounds.⁷⁸ Finally, MD simulations have highlighted the importance of accounting for dynamics within these complex systems. For example, Singh et al. created a biphasic model system containing oil and IL that correlated higher diffusion coefficients for TH/DBT in oil with higher rates of extraction into the ILs.⁸¹

3.4. MD Methodology Recommendations

The largest contributor in determining the accuracy of MD simulations is the choice of force field employed. Early ionic liquid force fields had multiple shortcomings that included poor solvent dynamics, incorrect reproduction of hydrogen bonding strength, and errors in solvent organization.⁹⁷ At the time of these parameterization efforts, ca. 2001-2010, the availability of experimental data for parameter validation was extremely limited and often conflicting.⁹⁸ However, as IL experimental measurements became more accurate, abundant, and reproducible over the past decade, the quality of nonpolarizable IL force fields improved considerably.^{99, 100} Polarizable ionic liquid models, such as CL&Pol,¹⁰¹ have been shown to provide major improvements to the description of dynamics in MD simulations⁷⁴ and can certainly be recommended for IL-mediated EDS studies. However, routinely employing polarizable force fields may be challenging given their sizable computing requirements. Alternatively, nonpolarizable IL force fields that scale atomic charges (e.g., by ± 0.8), such as the 0.8*OPLS-2009IL,⁹⁸ mimic the average charge screening caused by polarization and account for charge transfer effects in a cost-effective manner. More advanced parameterization schemes for nonpolarizable IL force fields have been reported, such as the OPLS-VSIL⁸⁸ that was guided by free energy of hydration calculations and uses a ‘virtual site’ centered within the imidazolium moiety that offloads negative charge to inside the plane of the ring. OPLS-

VSIL was validated against experiment and high-level ab initio molecular dynamics simulations^{99, 100} and has provided accurate results in MD studies by Yue et al.⁸⁰ and Verlarde-Salcedo et al.⁷⁹ for multiple IL-mediated EDS systems. Another potential alternative is the use of a first-principles force field that more accurately captures physical interactions,¹⁰² such as that by Choi et al. who developed parameters for [C₄MIM][BF₄] from first-principles calculations utilizing symmetry-adapted perturbation theory (SAPT).¹⁰³ Beyond force fields, the conditions under which MD simulations are performed contribute heavily to accuracy. To this end, Gabl et al. have reported a recommended best practices study for ionic liquid MD simulations, e.g., minimum of 20-30 ns and 500 ion pairs for correct dynamics.¹⁰⁴

Table 5. Key Findings of Ionic Liquid-Mediated Extractive Desulfurization Derived from COSMO calculations.

Year	# ILs Examined	Top ILs Identified	Key Findings	Ref.
2009	264	[C ₁ MIM][BF ₄], [C ₁ MIM][PF ₆]	Smaller cations with shorter alkyl chains gave higher selectivity for TH, but lower capacity. Anion size had no effect on selectivity, but larger anion volumes increased capacity.	¹⁰⁵
2011	168	[C ₂ C ₁ Mor][SCN]	Position of a heteroatom (O, N, and S) within the N-heterocyclic cation had an appreciable influence on IL's selectivity and capacity for TH, BT, & DBT	¹⁰⁶
2015	1860	[C ₆ MPy][NTf ₂]	Nonpolar cations with long alkyl chains and polar anions with strong hydrogen bonding and long alkyl chains have higher capacity and stronger affinity with TH/DBT.	¹⁰⁷
2015	210	[C ₄ MIM][H ₂ PO ₄]	Expanded criteria to examine IL solubility in the raffinate phase. Imidazolium class yielded the lowest solubility, but anion had a strong influence.	¹⁰⁸
2017	36260	[(MeOC ₃)Py][HCOO] [C ₂ MPy][Lac]	Multistage screening procedure for ILs that included COSMO, group contributions (GC), raffinate solubility, and Aspen Plus.	¹⁰⁹
2019	19300	[C ₄ MIM][OAc][NO ₃] [C ₄ MIM][OAc][SCN]	Multistage screening of double salt ionic liquids (DSILs) for TH/n-octane separation.	¹¹⁰

4. Conductor-Like Screening Model (COSMO)

Another powerful tool which is commonly used alongside QM calculations is the Conductor-Like Screening Model (COSMO), a dielectric continuum solvation approach that simulates solvent effects by approximating electrostatic interactions with a solute molecule.¹¹¹ An extension of the model for realistic solvation, COSMO-RS, incorporates a statistical thermodynamics treatment of interacting surfaces¹¹² that can aid in the rapid identification of potential IL solvents possessing efficient extraction properties and high selectivity for refractory sulfur compounds (Table 5).¹¹³ While the existing COSMO database contains the screening charge density distributions (i.e., σ -profiles) for a large number IL-forming cations and anions, any missing solvents can be readily derived using standard DFT calculations.

One of the earliest applications of COSMO-RS for IL-EDS screening was carried out by Banerjee and coworkers where 264 unique cation-anion combinations were screened as potential solvents for extracting TH from a simulated diesel model (i.e., *n*-hexane, cyclohexane, *i*-octane, toluene, TH, and DBT).¹⁰⁵ The ILs examined were composed from 11 cations, that included [C_nMIM] (*n* = 1, 2, 4, 6, 8), [C_nPy] (*n* = 2, 4, 6, 8), 1-octylquinolium [C₈QU], and 24 anions with the COSMO files for the cations and anions generated separately using PBV86. The extractive ability of each IL was examined in terms of solute capacity and selectivity towards TH over fuel components. Interestingly a competing effect between selectivity and capacity was found to be dependent on the size of the cation, including the length of the alkyl side chain group. Smaller cations gave a higher selectivity, but a lower capacity compared to larger cations. For example, the 5-membered [C_nMIM] ring was found to be more selective for TH than the 6-membered rings of [C_nPy] and [C₈QU], though the larger cations could accommodate a greater amount of TH. Problematically, the larger volume channels present within these ILs composed of bigger cations are also capable of solvating straight chain fuel components reducing the selectivity for TH and potentially lowering the fuel octane number.

Interestingly, no selectivity trend was noted due to increasing anion volume, but the capacity did increase with increasing anion size. Overall, a small imidazolium cation, e.g., [C₁MIM], coupled to the fluorinated anions [BF₄] and [PF₆] yielded the best extractive performance. Follow up work by the same team expanded their COSMO-RS study to 168 cation-anion combinations that featured additional classes of N-heterocyclic cations including pyrrolidinium, piperidinium, morpholinium, and pyrazolium.¹⁰⁶ The position of the heteroatom (O, N, and S) within the cation had an appreciable influence on IL's selectivity and capacity for TH, BT, and DBT.

With these key IL-EDS structural trends further verified,^{108, 114} later works focused on expanding the scope of COSMO to screen successively larger combinations of novel IL species. For example, Gao et al. systematically explored 1860 possible IL combinations (30 anions and 62 cations) for TH and DBT extraction by examining the influence of cation/anion structure, alkyl chain length, symmetry, and functional groups present.¹⁰⁷ The capacity of the IL was found to be highly dependent on the cation and anion species with a very wide range reported, e.g., 10⁻³–10¹ for TH and 10⁻³–10² for DBT. Hydrogen bonding and van der Waals interactions between TH/DBT and ILs dominated the contribution to capacity. Specifically, symmetrical cations with longer alkyl chains (up to C₁₂) and anions with higher polarity and longer alkyl chains provided the highest capacity ILs for TH/DBT. Despite all the success applying COSMO-RS in IL-EDS solvent screening, most research efforts to that point had primarily focused on extractive capacity and selectivity of the prospective extractant. However, another major area of importance in EDS is IL solubility in the raffinate phase as an excessive amount of molten salt remaining in the oil phase after completion of the extraction process will lead to a reduction in product quality. In response, Song et al. successfully employed COSMO-RS to examine 6 cations and 35 anion combinations with an expanded criteria that examined both IL solubility in the raffinate phase (i.e., heptane and toluene) and extractive ability.¹⁰⁸ Of

the cations studied, the imidazolium class yielded the lowest solubility in hydrocarbon, however the choice of anion had a stronger influence on the IL solubility. When considering an idealized balance of (1) extractive capacity, (2) TH selectivity, and (3) IL solubility, the most efficient cation-anion combination was predicted to be $[C_4MIM][H_2PO_4]$ and, accordingly, experimental examination confirmed high EDS performance.¹⁰⁸ Their results offer confidence that COSMO-RS screening of ILs can be an excellent predictive tool in the face of limited experimental data for IL solubility in solvent-sensitive systems.

The criteria for selecting new ILs in the EDS process can be enhanced beyond the thermodynamic properties computed with COSMO-RS through the addition of group contribution (GC) methods for the prediction of physical properties (e.g., viscosity and melting point) and the use of Aspen Plus¹¹⁵ to simulate process performance (e.g., operating conditions and solvent/energy consumption). For example, Song et al. utilized a new, stricter mass-based equilibrium cutoff for TH extraction from *n*-octane that favored ILs with lower atomic weights, at which stoichiometric ratios are easier to process.¹⁰⁹ They examined a pool of 36,260 IL pairs (370 cations and 98 anions) and, of these potential extractants, only 831 combinations were predicted to have higher extraction efficiencies than sulfolane, a benchmark conventional solvent for EDS. Additional constraints applied using GC methods, i.e., an upper bound melting point constraint of 298.15 K and a viscosity below 100 cP, narrowed the prospective ILs to 15 candidates composed of highly-alkylated imidazolium, pyridinium, and pyrrolidinium cations and carboxylate anions. Further refinement to ILs possessing low solubility in the raffinate phase reduced the number of solvents to four and a final screening with Aspen Plus revealed two ideal candidates for EDS: 1-(3-methoxypropyl)pyridinium formate, $[(MeOC_3)Py][HCOO]$, and 1-ethyl-3-methylpyridinium lactate, $[C_2MPy][Lac]$.¹⁰⁹ Further reinforcing this systematic approach, the same team employed a similar procedure to examine 19,300 double salt ionic liquids (DSILs) composed of more than one cation and/or

anion for TH/n-octane separation.¹¹⁰ Mixtures of [C₄MIM][OAc] with either [NO₃] or [SCN] were found to be the most promising DSILs with successful experimental validation of the solvents' extractive ability emphasizing the reliability of this multistep COSMO-RS based technique.¹¹⁰

It is evident that COSMO and other thermodynamic models can play a valuable and complementary role in identifying new extractants. The method's scalability allows for the facile coarse screening of IL pairs several orders of magnitude higher than solely using a QM or MD approach. While trends in structure-function properties can only be hypothesised, these models have nevertheless provided close agreement with experimental, QM, and MD findings. These include establishing that longer alkyl chains^{33, 54, 105-107, 116} and larger, more nonpolar nitrogen heterocyclic cations enhance extraction efficiency,^{45, 105, 107} while expanding upon QM and MD findings by identifying that a loss of selectivity is an important trade-off when diverging from imidazolium-based ILs.^{105, 107} Findings that sterically bulky,¹⁰⁵ highly polar,^{107, 108} hydrogen bond accepting anions^{105, 107-109} promote extraction efficiency has also been highlighted by QM and MD, with the latter methods highlighting both the importance of direct hydrogen-bonding to the C₂ carbon^{41, 43} (Figure 2) and packing modulation.^{76, 78, 80, 81} More recent COSMO findings have pushed the EDS field towards new classes of ILs that include double salt ILs¹¹⁰ and bio-ionic liquids.¹¹⁷

5. Future Directions

5.1. Coarse-Grained Molecular Dynamics (CGMD)

While MD serves as good model for representing bulk solvent effects in IL-mediated EDS processes, the simulations can quickly become intractable with increasing size and complexity, e.g., fuel oil mixtures composed of various aliphatic and aromatic hydrocarbons, or at dramatically longer time scales. Coarse-grain molecular dynamics (CGMD) can overcome

these limitations through a reduction in the model resolution that leaves fewer particles to compute and permits the use of larger integration time steps.¹¹⁸ CG models function by grouping set of atoms within a molecule into “beads”, e.g., see Figure 8 for $[\text{C}_2\text{MIM}][\text{NO}_3]$.¹¹⁹ Like conventional MD, CGMD requires extensive and well-planned parameterization of the beads to faithfully replicate the key physical processes being studied.¹¹⁸ Development of CG force fields for pure ILs began in 2005 by Wang and Voth¹²⁰ with continual improvements, such as transferability¹²¹ and polarization,¹²² reported by the CGMD community over the next two decades. While the use of CGMD to study IL-mediated EDS has not been reported to-date, Vainikka et al. have reported the first parameterization and simulation of a CG model for a deep eutectic solvent (DES) composed of tetrabutylammonium chloride and acetic acid (TBAC-AcAc) to study DES-mediated EDS.¹²³ A system consisting of 3000 octane molecules (model fuel), 30 BT, 30 2-methylthiophene (2-MTH), 600 TBAC, and 1200 AcAc were used to explore the origin of DES-enhanced desulfurization. The CGMD simulations predicted the extraction to be driven by $\text{CH}\cdots\pi$ interactions between TBAC and BT/2-MTH, which may be due in part to CG parameters designed to partially capture this interaction.¹²³ However, hydrogen bonding has been experimentally reported to play a major role in DES-mediated EDS,¹²⁴ suggesting the need for further refinement of this preliminary CG model. Nevertheless, the high efficiency and reasonable accuracy reported for CGMD in their DES-EDS study¹²³ emphasizes the future role that this promising technique could play in the rapid screening of new ILs for EDS.

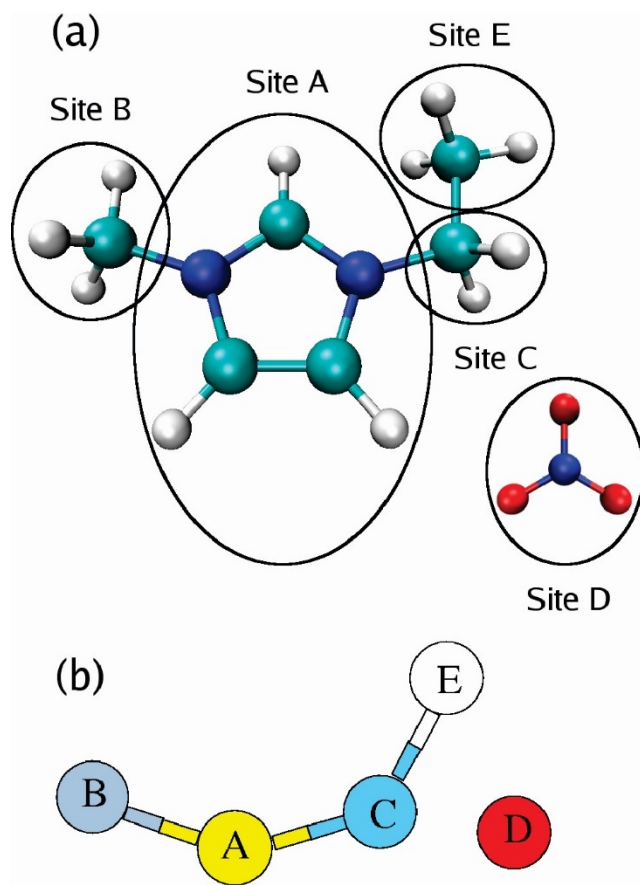


Figure 8. Coarse-graining scheme for [C₂MIM][NO₃], where (a) is the atomistic structure and (b) is the coarse-grained structure of the IL cation and anion. Reproduced with permission from ref. 119. Copyright 2007 American Chemical Society.

5.2. Ab Initio Molecular Dynamics (AIMD)

MD simulations have proven to be a powerful method for elucidating the microscopic organizational structure of refractory sulfur compounds in bulk phase ILs, but their utility is limited by several factors including (1) the fundamental force field framework that requires the development of parameters specific to the system under study, (2) no explicit accounting of electronic effects, e.g., charge transfer and HOMO-LUMO gap, and (3) the inability to describe chemical reactivity, such as oxidative reactions in IL-catalyzed ODS. While some of those limitations can be remediated by using more advanced MD methodologies, an alternative in the form of ab initio molecular dynamics (AIMD) has been shown to be an excellent tool in

the study of ILs.^{99, 125} AIMD propagates atoms through classical mechanics, but computes the forces “on the fly” through an electronic structure method, such as DFT, where electronic orbitals are expanded in a plane-wave basis set.¹²⁶ AIMD opens up study to virtually any IL-mediated EDS system of interest, e.g., magnetic ILs,⁹⁰ as a lack of available force field parameters is no longer constraining. However, the AIMD calculations are ultimately restricted in accuracy by the DFT method chosen, so following recent recommendations by Perit et al. for IL systems is advised.¹²⁷ In addition, the large computational cost required to perform AIMD often limits simulations to short timescales of ~100 ps using smaller systems of ~30 IL ion pairs, which ultimately restricts the amount of conformational space sampled and prohibits description of medium-to-long range structural order. Nevertheless, Velarde-Salcedo et al. successfully employed AIMD simulations for the computational EDS study of TH in four ILs composed of [C₄MIM] with [Cl], [Br], [BF₄], and [CH₃COO].⁷⁹ Their AIMD simulations were performed for TH and 30 IL ion pairs over a total period of 27-35 ps using the CP2K package.¹²⁸ RDF analysis of the AIMD simulations found smaller distances between TH and the IL anions, and presumably stronger interactions, compared to the IL cations. In addition, π - π stacking was observed at distances of 3.4 to 4.5 Å for the ILs with smaller anions, i.e., [Cl], [Br], and [BF₄], compared to [C₄MIM][CH₃COO] that gave longer π - π stacking distances of 4.5 to 6 Å enabling additional C \cdots π interactions between the TH ring and the alkyl chain of the cation. Finally, the AIMD simulations identified some weak-to-medium strength hydrogen bonds present between the S atom of TH and the ring protons of [C₄MIM] that were either underestimated or absent when employing classical MD simulations.⁷⁹

6. Conclusions

Ionic liquids have proven to be excellent extractant solvents capable of selectively removing refractory sulfur compounds from fuel oils while remaining unreactive with the desirable hydrocarbons.¹⁶ However, despite hundreds of promising experimental studies over

the past two decades, IL-mediated EDS has unfortunately faced significant challenges scaling to the industrial level.¹²⁹ This speaks to the need for new ILs with high recyclability, low cost, and physiochemical properties optimized for efficient desulfurization of fuel and oils. However, the near limitless combinations of ions capable of forming ILs³² presents a substantial challenge for rational design. Computational techniques can play a key role in this process with their ability to scrutinize and unravel the myriad of subtle interactions present between IL ions and sulfur impurities at the atomic level. COSMO-RS and other thermodynamical models have successfully identified potential IL extractants through efficient screening of tens of thousands of solvents. QM calculations have proven to be a powerful method for identifying and quantifying the outsized role played by π - π stacking, C-H \cdots π interactions, dispersion, and hydrogen bonding between the IL ions and the sulfur compounds. MD simulations have highlighted the necessity of bulk-phase solvent to be considered in the desulfurization process by emphasizing the importance of diffusion and the availability of free volume within the solvent. Continual advances in computational methodologies, e.g., improved force fields for MD simulations and dispersion corrections to DFT calculations, have provided a more accurate representation of the IL environment. Future investigations could benefit from highly efficient models, such as CGMD, capable of representing large and complex fuel oil mixtures or could employ more physically rigorous methods, like AIMD, that can incorporate electronic effects into dynamical simulations. In summary, computational studies have provided substantial advancement in understanding IL-mediated EDS over the past decade and have demonstrated the synergy with experiment necessary to tackle this difficult challenge.

Biographies

Orlando Acevedo is a Professor of Chemistry at the University of Miami. He received his Ph.D. in Computational Organic Chemistry at Duquesne University in 2003 and was a Postdoctoral Associate at Yale University from 2003-2006. He was an Assistant/Associate

Professor of Chemistry at Auburn University from 2006-2015 and moved to the University of Miami in 2015. His research program focuses upon the development of computational tools targeting the creation and purification of biofuels using ionic liquids.

Robert Wilson-Kovacs is a graduate student at the University of Miami. He received his MSci in Chemistry at the University of Bristol in 2018 and continued to study there until 2020 for his MRes in Chemistry specialising in self-assembled functional materials. Since joining the Acevedo group in 2021, he has worked with both quantum mechanical and molecular dynamics methods, with a particular focus on the dynamics of nano- and mesoscale systems.

Acknowledgements

Gratitude is expressed to the National Science Foundation (CHE-2102038) for support of this research.

Glossary

[C_nMIM] = 1-Alkyl-3-methylimidazolium

[MIM] = 1-methylimidazolium

[BzMIM] = 3-Benzyl-1-methylimidazolium

[*p*-NO₂BzMIM] = 3-(*p*-Nitro benzyl)-1-methylimidazolium

[*m*-NO₂BzMIM] = 3-(*m*-Nitro benzyl)-1-methylimidazolium

[*o*-NO₂BzMIM] = 3-(*o*-Nitro benzyl)-1-methylimidazolium

[C₄C₁MIM] = 1-Butyl-2,3-dimethylimidazolium

[C_nPy] = 1-Alkylpyridinium

[AMPy] = 1-Allyl-3-methylpyridinium

[C_nMPy] = 1-Alkyl-3-methylpyridinium

[(MeOC₃)Py] = 1-(3-Methoxypropyl)pyridinium

[C₄C₁Pyrr] = 1-Butyl-1methylpyrrolidinium

[C₂C₁Mor] = 4-Ethyl-4-methylmorpholinium

[TBHEP] = tri-*n*-Butyl-(2-hydroxyethyl)phosphonium

[TBCMP] = Tributyl(carboxymethyl)phosphonium

[NTf₂] = bis-(Trifluoromethylsulfonyl)imide

[OTf] = Trifluoromethanesulfonate

[TFA] = Trifluoroacetate

[Lac] = Lactate

HDS = Hydrodesulfurization

EDS = Extractive Desulfurization

ODS = Oxidative Desulfurization

TH = Thiophene

THO₂ = Thiophene sulfone

BT = Benzothiophene

DBT = Dibenzothiophene

DBTO₂ = Dibenzothiophene sulfone

DMDBT = dimethyldibenzothiophene

IL = Ionic Liquid

DFT = Density Functional Theory

NBO = Natural Bond Order

AIM = Atoms in Molecules

MD = Molecular Dynamics

AIMD = Ab Initio Molecular Dynamics

CGMD = Coarse-Grained Molecular Dynamics

References

- (1) X. Solomon, S.; Plattner, G.-K.; Knutti, R.; Friedlingstein, P. Irreversible climate change due to carbon dioxide emissions. *PNAS* **2009**, *106*, 1704-1709.
- (2) *World Health Organization: Air Pollution (Impact)*. https://www.who.int/health-topics/air-pollution#tab=tab_2 (accessed 2024 October).
- (3) Yorifuji, T.; Kashima, S.; Suryadhi, M. A. H.; Abudureyimu, K. Acute exposure to sulfur dioxide and mortality: Historical data from Yokkaichi, Japan. *Arch. Environ. Occup. Health* **2019**, *74*, 271-278. DOI: 10.1080/19338244.2018.1434474
- (4) Singh, A.; Agrawal, M. Acid rain and its ecological consequences. *J. Environ. Biol.* **2008**, *29*, 15-24.
- (5) Smith, S.; van Aardenne, J.; Klimont, Z.; Andres, R. J.; Volke, A.; Arias, S. D. Anthropogenic Sulfur Dioxide Emissions: 1850-2005. *Atmospheric Chemistry and Physics* **2011**, *11*, 1101-1116.
- (6) Soleimani, M.; Bassi, A.; Margaritis, A. Biodesulfurization of Refractory Organic Sulfur Compounds in Fossil Fuels. *Biotechnol. Adv.* **2007**, *25*, 570-596.

(7) Han, Y.; Zhang, Y.; Xu, C.; Hsu, C. S. Molecular Characterization of Sulfur-Containing Compounds in Petroleum. *Fuel* **2018**, *221*, 144-158.

(8) Shang, H.; Du, W.; Liu, Z.; Zhang, H. Development of Microwave Induced Hydrodesulfurization of Petroleum Streams: A Review. *J. Ind. Eng. Chem.* **2013**, *19*, 1061-1068.

(9) Zhao, H.; Baker, G. A. Oxidative Desulfurization of Fuels Using Ionic Liquids: A Review. *Front. Chem. Sci. Eng.* **2015**, *9*, 262-279. DOI: 10.1007/s11705-015-1528-0

(10) Wang, P.; Wang, R.; Matulis, V. E. Ionic Liquids as Green and Efficient Desulfurization Media Aiming at Clean Fuel. *Int. J. Environ. Res. Public Health* **2024**, *21*, 914.

(11) Faria, R. G.; Silva, D.; Mirante, F.; Gago, S.; Cunha-Silva, L.; Balula, S. S. Advanced Technologies Conciliating Desulfurization and Denitrogenation to Prepare Clean Fuels *Catalysts* **2024**, *14*, 137.

(12) Ji, W.; Liu, H.; Mu, J.; Kong, J.; Wei, Z.; Wang, J.; Wang, H.; Zhu, J. Insights into Ionic Liquids for Oil Desulfurization: A Study Based on Bibliometric Mapping. *Industrial & Engineering Chemistry Research* **2024**, *63*, 13421-13434. DOI: 10.1021/acs.iecr.4c01964.

(13) Qiu, X.; Wang, B.; Wang, R.; Kozhevnikov, I. V. New Adsorption Materials for Deep Desulfurization of Fuel Oil. *Materials* **2024**, *17*, 1803.

(14) Niu, A.; Xu, H.; Yuan, Q.; Wu, F.; Wei, X. Metal-based Ionic Liquids and Solid-loaded Catalysts in Fuel Oil Desulfurization: A Review. *Mini-Rev. Org. Chem.* **2024**, *21*, 704-716.

(15) Jha, D.; Maheshwari, P.; Singh, Y.; Haider, M. B.; Kumar, R.; Balathanigaimani, M. S. A Comparative Review of Extractive Desulfurization Using Designer Solvents: Ionic liquids & Deep Eutectic Solvents. *J. Energy Inst.* **2023**, *110*, 101313.

(16) Hosseini, A.; Khoshhsima, A.; Sabzi, M.; Rostam, A. Toward Application of Ionic Liquids to Desulfurization of Fuels: A Review. *Energy & Fuels* **2022**, *36*, 4119-4152.

(17) Aghaei, A.; Sobati, M. A. Extraction of Sulfur Compounds from Middle Distillate Fuels Using Ionic Liquids and Deep Eutectic Solvents: A Critical Review. *Fuel* **2022**, *310*, 122279.

(18) Desai, K.; Dharaskar, S.; Khalid, M.; Gedam, V. Effectiveness of ionic liquids in extractive-oxidative desulfurization of liquid fuels: a review. *Chemical Papers* **2022**, *76*, 1989–2028.

(19) Tanimu, A.; Tanimu, G.; Ganiyu, S. A.; Gambo, Y.; Alasiri, H.; Alhooshani, K. Metal-Free Catalytic Oxidative Desulfurization of Fuels—A Review. *Energy & Fuels* **2022**, *36*, 3394-3419. DOI: 10.1021/acs.energyfuels.1c04411.

(20) Paucar, N. E.; Kiggins, P.; Blad, B.; De Jesus, K.; Afrin, F.; Pashikanti, S.; Sharma, K. Ionic Liquids for the Removal of Sulfur and Nitrogen Compounds in Fuels: a Review. *Environ. Chem. Lett.* **2021**, *19*, 1205-1228.

(21) Malolan, R.; Gopinath, K. P.; N. Vo, D.-V.; Jayaraman, R. S.; Adithya, S.; Ajay, P. S.; Arun, J. Green Ionic Liquids and Deep Eutectic Solvents for Desulphurization, Denitrification, Biomass, Biodiesel, Bioethanol and Hydrogen Fuels: a Review. *Environ. Chem. Lett.* **2021**, *19*, 1001-1023.

(22) Lima, F.; Branco, L. C.; Silvestre, A. J. D.; Marrucho, I. M. Deep desulfurization of fuels: Are deep eutectic solvents the alternative for ionic liquids? *Fuel* **2021**, *293*, 120297.

(23) Boshagh, F.; Rahmani, M.; Rostami, K.; Yousefifar, M. Key Factors Affecting the Development of Oxidative Desulfurization of Liquid Fuels: A Critical Review. *Energy & Fuels* **2021**, *36*, 98-132. DOI: 10.1021/acs.energyfuels.1c03396.

(24) Ahmadian, M.; Anbia, M. Oxidative Desulfurization of Liquid Fuels Using Polyoxometalate-Based Catalysts: A Review. *Energy & Fuels* **2021**, *35*, 10347-10373. DOI: 10.1021/acs.energyfuels.1c00862.

(25) Zolotareva, D.; Zazybin, A.; Rafikova, K.; Dembitsky, V. M.; Dauletbaev, A.; Yu, V. Ionic Liquids Assisted Desulfurization and Denitrogenation of Fuels. *Vietnam J. Chem.* **2019**, *57*, 133-163.

(26) Ibrahim, M. H.; Hayyan, M.; Hashim, M. A.; Hayyan, A. The role of ionic liquids in desulfurization of fuels: A review. *Renew. Sust. Energy Rev.* **2017**, *76*, 1534-1549.

(27) Zazybin, A. G.; Rafikova, K.; Yu, V.; Zolotareva, D.; Dembitsky, V. M.; Sasaki, T. Metal-containing ionic liquids: current paradigm and applications. *Russian Chemical Reviews* **2017**, *86*, 1254-1270. DOI: 10.1070/rer4743.

(28) Kumar, S.; Srivastava, V. C.; Nanoti, S. M. Extractive Desulfurization of Gas Oils: A Perspective Review for Use in Petroleum Refineries. *Separation & Purification Reviews* **2017**, *46*, 319-347. DOI: 10.1080/15422119.2017.1288633.

(29) Abro, R.; Abdeltawab, A. A.; Al-Deyab, S. S.; Yu, G.; Qazi, A. B.; Gao, S.; Chen, X. A Review of Extractive Desulfurization of Fuel Oils Using Ionic Liquids. *RSC Adv.* **2014**, *4*, 35302-35317.

(30) Katasonova, O. N.; Savonina, E. Y.; Maryutina, T. A. Extraction Methods for Removing Sulfur and Its Compounds from Crude Oil and Petroleum Products. *Russ. J. Appl. Chem.* **2021**, *94*, 441-436.

(31) Rogers, R. D.; Seddon, K. R. Chemistry. Ionic liquids--solvents of the future? *Science* **2003**, *302*, 792-793. DOI: 10.1126/science.1090313

(32) Niedermeyer, H.; Hallett, J. P.; Villar-Garcia, I. J.; Hunt, P. A.; Welton, T. Mixtures of ionic liquids. *Chem. Soc. Rev.* **2012**, *41*, 7780-7802. DOI: 10.1039/c2cs35177c

(33) Bosmann, A.; Datsevich, L.; Jess, A.; Lauter, A.; Schmitz, C.; Wasserscheid, P. Deep Desulfurization of Diesel Fuel by Extraction with Ionic Liquids. *Chem. Commun.* **2001**, 2494-2495. DOI: 10.1039/b108411a

(34) Zhang, S.; Zhang, Z. C. Novel Properties of Ionic Liquids in Selective Sulfur Removal from Fuels at Room Temperature. *Green Chem.* **2002**, *4*, 376-379.

(35) Becke, A. D. Density-functional thermochemistry. III. The role of exact exchange *J. Chem. Phys.* **1993**, *98*, 5648-5652.

(36) Lee, C.; Yang, W.; Parr, R. G. Development of the Colle-Salvetti correlation-energy formula into a functional of the electron density. *Phys. Rev. B* **1988**, *37*, 785-789.

(37) Zhao, Y.; Truhlar, D. G. The M06 suite of density functionals for main group thermochemistry, thermochemical kinetics, noncovalent interactions, excited states, and transition elements: two new functionals and systematic testing of four M06-class functionals and 12 other functionals. *Theor. Chem. Acc.* **2008**, *120*, 215-241.

(38) Ratcliff, L.; Mohr, S.; Huhs, G.; Deutsch, T.; Masella, M.; Genovese, L. Challenges in large scale quantum mechanical calculations. *WIREs Comput. Mol. Sci.* **2017**, *7*, e1290.

(39) Lü, R.; Qu, Z.; Yu, H.; Wang, F.; Wang, S. The electronic and topological properties of interactions between 1-butyl-3-methylimidazolium hexafluorophosphate/tetrafluoroborate and thiophene. *J. Mol. Graph. Model.* **2012**, *36*, 36-41.

(40) Lü, R.; Lin, J.; Qu, Z. Theoretical study on interactions between ionic liquids and organosulfur compounds. *Computational and Theoretical Chemistry* **2012**, *1002*, 49-58.

(41) Gu, P.; Lü, R.; Liu, D.; Lu, Y.; Wang, S. Exploring the nature of interactions among thiophene, thiophene sulfone, dibenzothiophene, dibenzothiophene sulfone and a pyridinium-based ionic liquid. *Phys. Chem. Chem. Phys.* **2014**, *16*, 10531-10538.

(42) Li, H.; Chang, Y.; Zhu, W.; Jiang, W.; Zhang, M.; Xia, J.; Li, H. A DFT Study of the Extractive Desulfurization Mechanism by [BMIM]⁺[AlCl₄]⁻ Ionic Liquid. *J. Phys. Chem. B* **2015**, *119*, 5995-6009.

(43) Niknam, M.; Vatanparast, M.; Shekaari, H. Theoretical Study of Interactions Between 1-Alkyl-3-Methylimidazolium Tetrafluoroborate and Dibenzothiophene: DFT, NBO and AIM Analysis. *J. Struct. Chem.* **2017**, *58*, 1296-1306.

(44) Patra, R. N.; Gardas, R. L. Effect of Nitro Groups on Desulfurization Efficiency of Benzyl-Substituted Imidazolium-Based Ionic Liquids: Experimental and Computational Approach. *Energy & Fuels* **2019**, *33*, 7659-7666.

(45) Player, L. C.; Chan, B.; Lui, M. Y.; Masters, A. F.; Maschmeyer, T. Toward an Understanding of the Forces Behind Extractive Desulfurization of Fuels with Ionic Liquids. *ACS Sustainable Chem. Eng.* **2019**, *7*, 4087-4093.

(46) Moghadam, F. R.; Azizian, S.; Kianpour, E.; Yarie, M.; Bayat, M.; Zolfigol, M. A. Green fuel through green route by using a task-specific and neutral phosphonium ionic liquid: A joint experimental and theoretical study. *Chemical Engineering Journal* **2017**, *309*, 480-488.

(47) Kianpour, E.; Azizian, S.; Yarie, M.; Zolfigol, M. A.; Bayat, M. A task-specific phosphonium ionic liquid as an efficient extractant for green desulfurization of liquid fuel: An experimental and computational study. *Chemical Engineering Journal* **2016**, *295*, 500-508.

(48) Tsuzuki, S.; Luthi, H. P. Interaction energies of van der Waals and hydrogen bonded systems calculated using density functional theory: Assessing the PW91 model. *J. Chem. Phys.* **2001**, *114*, 3949-3957.

(49) Castellano, O.; Gimon, R.; Sosun, H. Theoretical study of the σ - π and π - π interactions in heteroaromatic monocyclic molecular complexes of benzene, pyridine, and thiophene dimers: Implications on the resin-asphaltene stability in crude oil. *Energy & Fuels* **2011**, *25*, 2526–2541.

(50) Kumar, P. S. V.; Raghavendra, V.; Subramanian, V. Bader's Theory of Atoms in Molecules (AIM) and its Applications to Chemical Bonding. *J. Chem. Sci.* **2016**, *128*, 1527–1536.

(51) Glendening, E. D.; Landis, C. R.; Weinhold, F. Natural bond orbital methods. *WIREs Comput. Mol. Sci.* **2012**, *1*-42.

(52) Bernales, V. S.; Marenich, A. V.; Contreras, R.; Cramer, C. J.; Truhlar, D. G. Quantum mechanical continuum solvation models for ionic liquids. *J. Phys. Chem. B* **2012**, *116*, 9122-9129. DOI: 10.1021/jp304365v

(53) Mo, Y.; Song, L.; Lin, Y. Block-Localized Wavefunction (BLW) Method at the Density Functional Theory (DFT) Level. *J. Phys. Chem. A* **2007**, *111*, 8291–8301.

(54) Zhang, S. G.; Zhang, Q. L.; Zhang, Z. C. Extractive Desulfurization and Denitrogenation of Fuels Using Ionic Liquids. *Ind. Eng. Chem. Res.* **2004**, *43*, 614–622.

(55) Austin, A.; Petersson, G. A.; Frisch, M. J.; Dobek, F. J.; Scalmani, G.; Throssell, K. A. Density Functional with Spherical Atom Dispersion Terms. *J. Chem. Theory Comput.* **2012**, *8*, 4989-5007.

(56) Tomasi, J.; Mennucci, B.; Cammi, R. Quantum mechanical continuum solvation models. *Chem. Rev.* **2005**, *105*, 2999-3093. DOI: 10.1021/cr9904009

(57) Weingärtner, H. The Static Dielectric Constant of Ionic Liquids. *J. Mol. Liq.* **2014**, *192*, 185–190.

(58) Xu, H.; Han, Z.; Zhang, D.; Liu, C. Theoretical elucidation of the dual role of [HMIm]BF₄ ionic liquid as catalyst and extractant in the oxidative desulfurization of dibenzothiophene. *J. Mol. Catal. A Chem.* **2015**, *398* 297-303.

(59) Yuan, P.; Zhang, T. T.; Cai, A. F.; Cui, C. S.; Liu, H. Y.; Bao, X. J. Theoretical study on the mechanism of oxidative-extractive desulfurization in imidazolium-based ionic liquid. *RSC Adv.* **2016**, *6*, 74929-74936.

(60) Wang, H.; Xu, M.; Zhou, R. Mechanism of extractive/oxidative desulfurization using the ionic liquid inimidazole acetate: a computational study. *J. Mol. Model.* **2017**, *23*, 54. DOI: 10.1007/s00894-017-3230-2

(61) Acevedo, O. Simulating Chemical Reactions in Ionic Liquids Using QM/MM Methodology. *J. Phys. Chem. A* **2014**, *118*, 11653–11666.

(62) Lo, W. H.; Yang, H. Y.; Wei, G. T. One-pot desulfurization of light oils by chemical oxidation and solvent extraction with room temperature ionic liquids. *Green Chem.* **2003**, *5*, 639-642.

(63) Lu, L.; Cheng, S.; Gao, J.; Gao, G.; He, M.-Y. Deep Oxidative Desulfurization of Fuels Catalyzed by Ionic Liquid in the Presence of H₂O₂. *Energy & Fuels* **2007**, *21*, 383–384.

(64) Zhao, D.; Wang, Y.; Duan, E.; Zhang, J. Oxidation desulfurization of fuel using pyridinium-based ionic liquids as phase-transfer catalysts. *Fuel Process. Technol.* **2010**, *91*, 1803-1806.

(65) Zhao, D.; Sun, Z.; Li, F.; Liu, R.; Shan, H. Oxidative Desulfurization of Thiophene Catalyzed by (C4H₉)₄NBr·2C₆H₁₁NO Coordinated Ionic Liquid. *Energy & Fuels* **2008**, *22*, 3065-3069.

(66) Bhutto, A. W.; Abro, R.; Gao, S.; Abbas, T.; Chen, X.; Yu, G. Oxidative desulfurization of fuel oils using ionic liquids: A review. *J. Taiwan Inst. Chem. Eng.* **62**, 84-97.

(67) Liu, F.; Yu, J.; Qazi, A. B.; Zhang, L.; Liu, X. Metal-Based Ionic Liquids in Oxidative Desulfurization: A Critical Review. *Environ. Sci. Technol.* **2021**, *55*, 1419-1435. DOI: 10.1021/acs.est.0c05855

(68) Fukui, K.; Yonezawa, T.; Shingu, H. A Molecular Orbital Theory of Reactivity in Aromatic Hydrocarbons. *J. Chem. Phys.* **1952**, *20*, 722-725.

(69) Grimme, S.; Antony, J.; Ehrlich, S.; Krieg, H. A consistent and accurate ab initio parametrization of density functional dispersion correction (DFT-D) for the 94 elements H-Pu. *J. Chem. Theory. Comput.* **2010**, *132*, 154104.

(70) Seeger, Z. L.; Izgorodina, E. I. A Systematic Study of DFT Performance for Geometry Optimizations of Ionic Liquid Clusters. *J. Chem. Theory Comput.* **2020**, *16*, 6735–6753.

(71) Grimme, S. Density functional theory with London dispersion corrections. *WIREs Comput. Mol. Sci.* **2011**, *1*, 211-228.

(72) Boese, A. D. Density Functional Theory and Hydrogen Bonds: Are We There Yet? *ChemPhysChem* **2015**, *16*, 978-985.

(73) Riniker, S. Fixed-Charge Atomistic Force Fields for Molecular Dynamics Simulations in the Condensed Phase: An Overview. *J. Chem. Inf. Model.* **2018**, 565–578.

(74) Bedrov, D.; Piquemal, J. P.; Borodin, O.; MacKerell, A. D., Jr.; Roux, B.; Schroder, C. Molecular Dynamics Simulations of Ionic Liquids and Electrolytes Using Polarizable Force Fields. *Chem. Rev.* **2019**, *119*, 7940-7995. DOI: 10.1021/acs.chemrev.8b00763

(75) Hénin, J.; Lelièvre, T.; Shirts, M. R.; Valsson, O.; Delemonette, L. Enhanced Sampling Methods for Molecular Dynamics Simulations. *Living J. Comput. Mol. Sci.* **2022**, *4*, 1583-1642.

(76) Liu, X.; Zhou, G.; Zhang, X.; Zhang, S. Molecular Dynamics Simulation of Desulfurization by Ionic Liquids. *AIChE Journal* **2010**, *56*, 2983-2996.

(77) Oliveira, O. V.; Paluch, A. S.; Costa, L. T. A molecular understanding of the phase-behavior of thiophene in the ionic liquid [C₄mim]⁺[BF₄]⁻ for extraction from petroleum streams. *Fuel* **2016**, *175*, 225–231.

(78) Cheng, H.; Zhang, J.; Qi, Z. Effects of Interaction with Sulfur Compounds and Free Volume in Imidazolium-Based Ionic Liquid on Desulfurisation: a Molecular Dynamics Study. *Mol. Simul.* **2017**, *44*, 55-62.

(79) Velarde-Salcedo, M. V.; Sánchez-Badillo, J.; Gallo, M.; López-Lemus, J. Excess chemical potential of thiophene in [BMIM] [BF₄, Cl, Br, CH₃COO] ionic liquids, determined by molecular simulations. *RSC Adv.* **2021**, *11*, 29394-29406.

(80) Yue, K.; Acevedo, O. Uncovering the Critical Factors that Enable Extractive Desulfurization of Fuels in Ionic Liquids and Deep Eutectic Solvents from Simulations. *J. Phys. Chem. B* **2023**, *127*, 6354-6373.

(81) Singh, M. B.; Harmalkar, A. U.; Prabhu, S. S.; Pai, N. R.; Bhangde, S. K.; Gaikar, V. G. Molecular dynamics simulation for desulfurization of hydrocarbon fuel using ionic liquids. *J. Mol. Liquids* **2018**, *264*, 490-498.

(82) Wang, J.; Song, Z.; Li, X.; Cheng, H.; Chen, L.; Qi, Z. Toward Rational Functionalization of Ionic Liquids for Enhanced Extractive Desulfurization: Computer-Aided Solvent Design and Molecular Dynamics Simulation. *Ind. Eng. Chem. Res.* **2020**, *59*, 2093-2103.

(83) Daneshvar, A.; Moosavi, M. Molecular Dynamics Simulation of Extractive Desulfurization of Diesel Oil Model Using Magnetic Ionic Liquids. *Fluid Phase Equilibria* **2021**, *548*, 113189.

(84) Wang, J.; Wolf, R. M.; Caldwell, J. W.; Kollman, P. A.; Case, D. A. Development and testing of a general amber force field. *J. Comput. Chem.* **2004**, *25*, 1157-1174. DOI: 10.1002/jcc.20035

(85) Liu, Z.; Huang, S.; Wang, W. A refined force field for molecular simulation of imidazolium-based ionic liquids. *J. Phys. Chem. B* **2004**, *108*, 12978-12989.

(86) Hess, B.; Kutzner, C.; van der Spoel, D.; Lindahl, E. GROMACS 4: Algorithms for Highly Efficient, Load-Balanced, and Scalable Molecular Simulation. *J. Chem. Theory. Comput.* **2008**, *4*, 435-447. DOI: 10.1021/ct700301q

(87) Brouwer, T.; Schuur, B. Model Performances Evaluated for Infinite Dilution Activity Coefficients Prediction at 298.15 K. *Ind. Eng. Chem. Res.* **2019**, *58*, 8903-8914.

(88) Doherty, B.; Zhong, X.; Acevedo, O. Virtual Site OPLS Force Field for Imidazolium-Based Ionic Liquids. *J. Phys. Chem. B* **2018**, *122*, 2962-2974. DOI: 10.1021/acs.jpca.7b11996

(89) Velez, C.; Acevedo, O. Simulation of deep eutectic solvents: Progress to promises. *WIREs Comput. Mol. Sci.* **2022**, *12*, e1598.

(90) Figueiredo, N. M.; Voroshlyova, I. V.; Ferreira, E. S. C.; Marques, J. M. C.; Cordeiro, M. Magnetic Ionic Liquids: Current Achievements and Future Perspectives with a Focus on Computational Approaches. *Chem. Rev.* **2024**, *124*, 3392-3415. DOI: 10.1021/acs.chemrev.3c00678

(91) Ko, N. H.; Lee, J. S.; Huh, E. S.; Lee, H.; Jung, K. D.; Kim, H. S.; Cheong, M. Extractive Desulfurization Using Fe-Containing Ionic Liquids. *Energy & Fuels* **2008**, *22*, 1687-1690.

(92) J.-M., M.-M.; Oviedo-Roa, R.; Garcia, P.; Martinez-Palou, R. DFT study of the interaction between ethanethiol and Fe-containing ionic liquids for desulfurization of natural gasoline. *Fuel Process. Technol.* **2012**, *97*, 24-29.

(93) Li, H.; Zhu, W.; Chang, Y.; Jiang, W.; Zhang, M.; Yin, S.; Xia, J.; Li, H. Theoretical investigation of the interaction between aromatic sulfur compounds and [BMIM]⁺[FeCl₄]⁻ ionic liquid in desulfurization: A novel charge transfer. *J. Mol. Graph. Model.* **2015**, *59*, 40-49.

(94) Hayashi, S.; Hamaguchi, H.-O. Discovery of a Magnetic Ionic Liquid [Bmim]FeCl₄. *Chem. Lett.* **2004**, *33*, 1590-1591.

(95) Jewett, A. I.; Stelter, D.; Lambert, J.; Saladi, S. M.; Roscioni, O. M.; Ricci, M.; Autin, L.; Maritan, M.; Bashusqeh, S. M.; Keyes, T.; et al. Moltemplate: A Tool for Coarse-Grained Modeling of Complex Biological Matter and Soft Condensed Matter Physics. *J. Mol. Biol.* **2021**, *433*, 166841. DOI: 10.1016/j.jmb.2021.166841

(96) Thompson, A. P.; Aktulga, H. M.; Berger, R.; Bolintineanu, D. S.; Brown, W. M.; Crozier, P. S.; in't Veld, P. J.; Kohlmeyer, A.; Moore, S. G.; Nguyen, T. D.; et al. LAMMPS - a flexible simulation tool for particle-based materials modeling at the atomic, meso, and continuum scales. *Comput. Phys. Commun.* **2022**, *271*, 10817.

(97) Zahn, S.; Cybik, R. Comparison of four ionic liquid force fields to an ab initio molecular dynamics simulation. *Am. J. Nano Res. Appl.* **2014**, *2*, 19-26.

(98) Doherty, B.; Zhong, X.; Gathiaka, S.; Li, B.; Acevedo, O. Revisiting OPLS Force Field Parameters for Ionic Liquid Simulations. *J. Chem. Theory. Comput.* **2017**, *13*, 6131-6145. DOI: 10.1021/acs.jctc.7b00520

(99) Yue, K.; Doherty, B.; Acevedo, O. Comparison between Ab Initio Molecular Dynamics and OPLS-Based Force Fields for Ionic Liquid Solvent Organization. *J. Phys. Chem. B* **2022**, *126*, 3908-3919.

(100) Memar, Z. O.; Moosavi, M. Assessing OPLS-based force fields for investigating the characteristics of imidazolium-based dicationic ionic liquids: A comparative study with AIMD simulations and experimental findings. *J. Chem. Phys. J. Chem. Phys.* **2023**, *159*, 244504.

(101) Goloviznina, K.; Canongia Lopes, J. N.; Gomes, M. C.; Pádua, A. H. Transferable, Polarizable Force Field for Ionic Liquids. *J. Chem. Theory Comput.* **2019**, *15*, 5858-5871.

(102) Sun, L. D., W.-Q. Recent developments of first-principles force fields. *WIREs Comput. Mol. Sci.* **2017**, e1282.

(103) Choi, E.; McDaniel, J. G.; Schmidt, J. R.; Yethiraj, A. First-Principles, Physically Motivated Force Field for the Ionic Liquid [BMIM][BF₄]. *J. Phys. Chem. Lett.* **2014**, *5*, 2670-2674. DOI: 10.1021/jz5010945

(104) Gabl, S.; Schröder, C.; Steinhauser, O. Computational studies of ionic liquids: Size does matter and time too. *J. Chem. Phys.* **2012**, *137*, 094501.

(105) Kumar, A. A. P.; Banerjee, T. Thiophene separation with ionic liquids for desulphurization: A quantum chemical approach. *Fluid Phase Equilibria* **2009**, *278*, 1-8. DOI: 10.1016/j.fluid.2008.11.019.

(106) Anantharaj, R.; Banerjee, T. COSMO-RS based predictions for the desulphurization of diesel oil using ionic liquids: Effect of cation and anion combination. *Fuel Process. Technol.* **2011**, *92*, 39-52. DOI: 10.1016/j.fuproc.2010.08.018.

(107) Gao, S.; Chen, X.; Abro, R.; Abdeltawab, A. A.; Al-Deyab, S. S.; Yu, G. Desulfurization of Fuel Oil: Conductor-like Screening Model for Real Solvents Study on Capacity of Ionic Liquids for Thiophene and Dibenzothiophene. *Ind. Eng. Chem. Res.* **2015**, *54*, 9421-9430. DOI: 10.1021/acs.iecr.5b01385.

(108) Song, Z.; Zhou, T.; Zhang, J.; Cheng, H.; Chen, L.; Qi, Z. Screening of ionic liquids for solvent-sensitive extraction –with deep desulfurization as an example. *Chemical Engineering Science* **2015**, *129*, 69-77. DOI: 10.1016/j.ces.2015.02.023.

(109) Song, Z.; Zhou, T.; Qi, Z.; Sundmacher, K. Systematic Method for Screening Ionic Liquids as Extraction Solvents Exemplified by an Extractive Desulfurization Process. *ACS Sustainable Chem. Eng.* **2017**, *5*, 3382-3389. DOI: 10.1021/acssuschemeng.7b00024.

(110) Song, Z.; Hu, X.; Zhou, Y.; Zhou, T.; Qi, Z.; Sundmacher, K. Rational design of double salt ionic liquids as extraction solvents: Separation of thiophene/n-octane as example. *AIChE Journal* **2019**, *65*. DOI: 10.1002/aic.16625.

(111) Klamt, A.; Schüürmann, G. COSMO: a new approach to dielectric screening in solvents with explicit expressions for the screening energy and its gradient. *J. Chem. Soc., Perkin Trans. 2* **1993**, 799-805. DOI: 10.1039/p29930000799.

(112) Klamt, A. Conductor-like Screening Model for Real Solvents: A New Approach to the Quantitative Calculation of Solvation Phenomena. *J. Phys. Chem.* **2002**, *99*, 2224-2235. DOI: 10.1021/j100007a062.

(113) Klamt, A. The COSMO and COSMO-RS solvation models. *WIREs Comput. Mol. Sci.* **2017**, *8*. DOI: 10.1002/wcms.1338.

(114) Devi Wilfred, C.; Man, Z.; Phak Chan, Z. Predicting methods for sulfur removal from model oils using COSMO-RS and partition coefficient. *Chemical Engineering Science* **2013**, *102*, 373-377. DOI: 10.1016/j.ces.2013.08.032.

(115) *Aspen Plus v14*, Aspen Technology Inc, Bedford, MA, USA; **2024**.

(116) Nancarrow, P.; Mustafa, N.; Shahid, A.; Varughese, V.; Zaffar, U.; Ahmed, R.; Akther, N.; Ahmed, H.; AlZubaidy, I.; Hasan, S.; et al. Technical Evaluation of Ionic Liquid-Extractive Processing of Ultra Low Sulfur Diesel Fuel. *Ind. Eng. Chem. Res.* **2015**, *54*, 10843-10853. DOI: 10.1021/acs.iecr.5b02825.

(117) Santiago, R.; Díaz, I.; González-Miquel, M.; Navarro, P.; Palomar, J. Assessment of bio-ionic liquids as promising solvents in industrial separation processes: Computational screening using COSMO-RS method. *Fluid Phase Equilibria* **2022**, *560*. DOI: 10.1016/j.fluid.2022.113495.

(118) Joshi, S. Y.; Deshmukh, S. A. A Review of Advancements in Coarse-Grained Molecular Dynamics Simulations. *Mol. Simul.* **2021**, *47*, 786-803.

(119) Wang, Y.; Jiang, W.; Yan, T.; Voth, G. A. Understanding Ionic Liquids through Atomistic and Coarse-Grained Molecular Dynamics Simulations. *Acc. Chem. Res.* **2007**, *1193–1199*.

(120) Wang, Y.; Voth, G. A. Unique Spatial Heterogeneity in Ionic Liquids. *J. Am. Chem. Soc.* **2005**, *127*, 12192-12193.

(121) Wang, Y.; Feng, S.; Voth, G. A. Transferable Coarse-Grained Models for Ionic Liquids. *J. Chem. Theory Comput.* **2009**, *5*, 1091-1098.

(122) Uhlig, F.; Zeman, J.; Smiatek, J.; Holm, C. First-Principles Parametrization of Polarizable Coarse-Grained Force Fields for Ionic Liquids. *J. Chem. Theory. Comput.* **2018**, *14*, 1471-1486. DOI: 10.1021/acs.jctc.7b00903

(123) Veinikka, P.; Thallmair, S.; Souza, P. C. T.; Marrink, S. W. Martini 3 Coarse-Grained Model for Type III Deep Eutectic Solvents: Thermodynamic, Structural and Extraction Properties. *ACS Sustainable Chem. Eng.* **2021**, *9*, 17338-17350.

(124) Li, C.; Li, D.; Zou, S.; Li, Z.; Yin, J.; Wang, A.; Cui, Y.; Yao, Z.; Zhao, Q. Extraction desulfurization process of fuels with ammonium based deep eutectic solvents. *Green Chem.* **2013**, *15*, 2793-2799.

(125) Del Popolo, M. G.; Lynden-Bell, R. M.; Kohanoff, J. Ab initio molecular dynamics simulation of a room temperature ionic liquid. *J. Phys. Chem. B* **2005**, *109*, 5895-5902. DOI: 10.1021/jp044414g

(126) Iftimie, R.; Minary, P.; Tuckerman, M. E. Ab initio molecular dynamics: concepts, recent developments, and future trends. *Proc. Natl. Acad. Sci. U.S.A* **2005**, *102*, 6654-6659. DOI: 10.1073/pnas.0500193102

(127) Perlt, E.; Ray, P.; Hansen, A.; Malberg, F.; Grimme, S.; Kirchner, B. Finding the best density functional approximation to describe interaction energies and structures of ionic liquids in molecular dynamics studies. *J. Chem. Phys.* **2018**, *148*, 193835. DOI: 10.1063/1.5013122

(128) Kühne, T. D.; al., e. CP2K: An electronic structure and molecular dynamics software package -Quickstep: Efficient and accurate electronic structure calculations. *J. Chem. Phys.* **2020**, *152*, 194103.

(129) Salah, H. B.; Nancarrow, P.; Al-Othman, A. Ionic liquid-assisted refinery processes - A review and industrial perspective. *Fuel* **2012**, *302*, 121195.

Table of Contents (TOC) Graphic

